STUDY OF 2 MICRON LASER

by

Seyed Hossein Hosseini

_____

A Thesis Submitted to the Faculty of the

JAMES C. WYANT COLLEGE OF OPTICAL SCIENCES

In Partial Fulfillment of the Requirements

For the Degree of

MASTER OF SCIENCE

In the Graduate College

THE UNIVERSITY OF ARIZONA

2022

THE UNIVERSITY OF ARIZONA
GRADUATE COLLEGE

As members of the Master's Committee, we certify that we have read the thesis prepared by **Seyed Hossein Hosseini**, titled ***Study of 2 Micron Laser*** and recommend that it be accepted as fulfilling the thesis requirement for the Master's Degree.

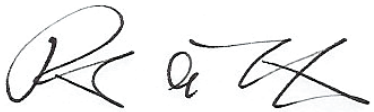

_____ Date: 08/10/22
Professor Robert A. Norwood

Mahmoud Fallahi

_____ Date: 8/11/22
Professor Mahmoud Fallahi

_____ Date: 8/11/22
Professor Xiushan Zhu

Final approval and acceptance of this thesis is contingent upon the candidate's submission of the final copies of the thesis to the Graduate College.

I hereby certify that I have read this thesis prepared under my direction and recommend that it be accepted as fulfilling the Master's requirement.

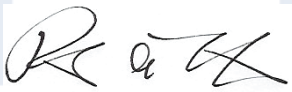

_____ Date: 8/11/22
Professor Robert A. Norwood
Master's Thesis Committee Chair
Wyant College of Optical Sciences

Acknowledgments

I would first like to express my especial and well-deserved appreciation to my advisor

Dr. Norwood.It was not possible to achieve my current accomplishments without his insightful instructions, priceless guidance, and great contributions to my research and studies. I have learned so many lessons from his behavior and advice. I firmly believe that I will remember how he has had played such an impressive professional role in my professional and personal life. Once again, I would like to thank Dr Norwood for his guidance, patience, support, faith, and for always being with me and his other students. I am also thankful to Dr. Xiushan Zhu for giving me permission working in his lab, Dr. Mahmoud Fallahi for accepting being in my committee, Dr. Masud Mansuripur for his support and advice, and Dr. Daewook Kim for giving me the opportunity to learn from him, as well as everyone in Wyant College of Optical Sciences, University of Arizona who provided a friendly and stimulating environment during my studies. I am deeply grateful to my lovely father and mother, brother and sister for their endless love and support. I am extremely thankful to my kind father and mother-in-law, my sister and brothers-in law for their prayerful support, patience, presence, and love. My wife and I are incredibly fortunate to have them in our life. Finally, of course, I am extremely thankful for the endurance and loving support from my lovely wife. She has been so supportive encouraging and understanding of me and my education. I am always indebted to her.

Contents

Abstract

Over the past decade, fiber lasers have developed in all aspects of laser performance with some significant advantages including excellent heat dissipation, single pass high gain, beam quality, freedom from alignment, compactness, and low maintenance. These advantages lead to different applications in material welding, soldering, marking, cleaning, medicine, research, security, etc.

Fiber lasers can work in a vast spectral range from deep UV to IR. The 2 μm region which is in mid IR has drawn tremendous attention for vawrious different applications. For instance, 2 μm lasers have smaller atmospheric scattering, atmospheric distortion and thermal blooming compared to 1 μm lasers, which lead to working more efficiently in light detection and ranging (LIDAR), direct energy laser weapon, sensing systems, and optical communication; 2 μm lasers are good candidates for non-metal material processing applications such as direct cutting, welding, and drilling. Especially, plastics are transparent in 1 μm region, while they have high absorption at 2 μm. The work presented in this thesis, includes demonstration of fiber laser using thulium

doped fiber at 1940 nm, fiber laser amplifier operating at the same wavelength and ; study of co-doped Tm^{3+} /Ho^{3+} fiber laser operating at 2050 nm; investigation of Q-switched fiber laser at 1940 nm using active Q-switching.

Chapter 1 Introduction

There is no doubt our daily life is impacted by photonics massively. Laser systems have a major influence in the photonics industry and modern technology. After the birth of the laser many activities in optics were created and developed into new scientific fields such as nonlinear optics, fiber optics, and opto-electronics which resulted in revitalizing this "ancient science". These days our lives are dependent on the science of laser physics and photonics, and it has been contributing to other fields, such as medical research, biology, information technology, MEMS, etc.

With all that being said, the search for developing new applications and improvements in technology is a never-ending process. A small part of this journey is to study different wavelength lasers for new applications. Recently, significant attention has been devoted to using thulium ions (Tm^3) generate radiation in the 1.9um to 2μm range, which is in eye safe region, and it has proven to be of great interest.

1.1 History

In early of 20th century, the relationship between energy and radiation frequency was found by a German theoretical physicist Max Planck. He found that light quanta constitute an energy that could be released or absorbed only in discrete packets, even though these pieces were ordinarily very small. Therefore, one can say his theory was a turning point in physics and his research inspired physicists such as Albert Einstein. Einstein in 1905, published a paper on the photoelectric effect, which stated that light can deliver its energy in chunks, in this case discrete quantum particles which nowadays are called photons.

In 1917, Albert Einstein confirmed the theoretical foundations based on the probability coefficients of absorption and emissions.[1] In 1928, Rudolf W. Ladenburg while confirming Einstein s'idea, deep rooted that emission can be in the form of stimulated emission and negative absorption.[2] In the next ten years, a Soviet scientist ,Valentin A. Fabrikant predicted the concept of short wave amplification by the use of stimulated emission.[3] followed by Willis E. Lamb and R.C. Rutherford discovering stimulated emission in hydrogen spectra in 1947.[2] Optical pumping was also proposed in 1950 which was experimentally confirmed later on Brussel, Kastler, and Winter.[4].

In 1953, Charles Hard Townes and graduate students James P. Gordon and Herbert J. Zeiger developed the very first microwave amplifier, although they couldn't generate continuous output. [5] Meanwhile, Basov and Prokhorov, two Soviet physicists, were independently working on the quantum oscillator and solved the problem of continuous-output systems. Later on, they proposed optical pumping of a multi-level system to create population inversion, which is a primary method of laser pumping.

In 1964 Charles H. Townes, Nikolay Basov, and Aleksandr Prokhorov won the Nobel Prize in Physics together, "for fundamental work in the field of quantum electronics, which has led to the construction of oscillators and amplifiers based on the maser–laser principle".

In 1957, Charles Hard Townes and Arthur Leonard Schawlow at Bell Labs started to study infrared lasers. As ideas developed, instead of completing their work on infrared radiation, they started working on visible light. It was in 1958 when Bell Labs filed a patent application for their proposed optical maser which was based on the work of Schawlow and Townes.

Simultaneously, graduate student Gordon Gould from Columbia University was working on his thesis regarding the energy levels of excited thallium. While working on his thesis, Gould met with Townes and their main discussions were about radiation emission. Afterwards, in November 1957, Gould noted his ideas for a "laser", which was using an open resonator. Furthermore, in 1958, in the USSR, Prokhorov suggested using an open resonator, which was the first published appearance of this idea. In the U.S., Schawlow and Townes had agreed to an open-resonator laser design, as they were apparently unaware of Prokhorov's publications and Gould's unpublished laser work.

At a conference in 1959, Gordon Gould published the term LASER in the paper The LASER, Light Amplification by Stimulated Emission of Radiation.[6][7] Gould's linguistic intention was using the "-aser" word particle as a suffix – to accurately denote the spectrum of the light emitted by the LASER device; thus x-rays: xaser, ultraviolet: uvaser, et cetera; none established itself as a discrete term, although "raser" was briefly popular for denoting radio-frequency-emitting devices.

Gould continued to develop the idea which resulted in a patent application being filed in April 1959. However, his application was denied by the U.S. Patent Office, and they awarded a patent to Bell Labs, in 1960. By doing so, a twenty-eight-years lawsuit was provoked, featuring scientific prestige and money as the stakes. As a result of the lawsuit Gould won his first minor patent in 1977, however, it was not until 1987 that he won the first significant patent lawsuit victory, when a federal judge ordered the U.S. Patent Office to issue patents to Gould for optically pumped and the gas discharge laser devices.[8]

Theodore H. Maiman demonstrated the first functioning laser on May 16, 1960[9][10] at Hughes Research Laboratories, Malibu, California, ahead of several research teams. He used a flash lamp-pumped synthetic ruby crystal to produce red laser light at 694 nm. Pulsed operation was only capable from this device, due to its three-level pumping design scheme. Later that year, an Iranian physicist Ali Javan, William R. Bennett, and Donald Herriot, created the very first gas laser, using helium and neon. It was capable of continuous operation in the infrared (U.S. Patent 3,149,290); later in 1993, Javan received the Albert Einstein Award. In 1962, Robert N. Hall operated the first laser diode using gallium arsenide and emitting at 850 nm.

The first experiments with Tm^{3+} and Ho^{3+} were done in 1960s. [11] The mid IR laser transition for both ions happened at upper Stark level of ground state. The first Tm:YAG laser at 2 μm using this transition was carried out by Johnson et al. in 1965, They used flashlight pump working at 77 K. The first pump laser operating at room temperature at 2 μm was done at 1975 by Caird et al. using Cr, Tm:YAG as the gain media.[12]

All in all, over the next 60 years, continual innovation has been seen in the field of laser physics which resulted in making lasers present in almost every aspect of everyday life. (https://en.wikipedia.org/wiki/Laser#Foundations)

1.2 Application

Over the past decade, fiber lasers have developed in all aspects of laser performance with some significant advantages including excellent heat dissipation, single pass high gain, beam quality, freedom from alignment, compactness, and low maintenance. These advantages lead to different applications in material welding, soldering, marking, cleaning, medicine, research, security, etc.

Fiber lasers can work in a vast spectral range from deep UV to IR. The 2 μm region which is in mid IR has drawn tremendous attention for various applications. For instance, 2 μm lasers have smaller atmospheric scattering, atmospheric distortion and thermal blooming compared to 1 μm lasers, which lead to working more efficiently in light detection and ranging (LIDAR), direct energy laser weapon, sensing systems, and optical communication; 2 μm lasers are good candidates for non-metal material processing applications such as direct cutting, welding, and drilling. Especially, plastics are transparent in 1 μm region, while they have high absorption at 2 μm [13]; They have also attracted much attention for highly precise laser surgery for both soft and hard tissue owing to a strong water absorption peak near 2 μm as shown in Fig. 1.1 [14]; 2 μm lasers can as also be utilized as pump sources for laser systems that operate at longer wavelengths in the mid-infrared or THz range [15,16]. Due to increasing demand for high energy lasers at 2 μm, significant efforts have been made to develop 2 μm lasers in the last decade and most research has been focused on thulium (Tm^{3+}) lasers due to strong absorption around 800 nm, where high-power laser diodes are available.

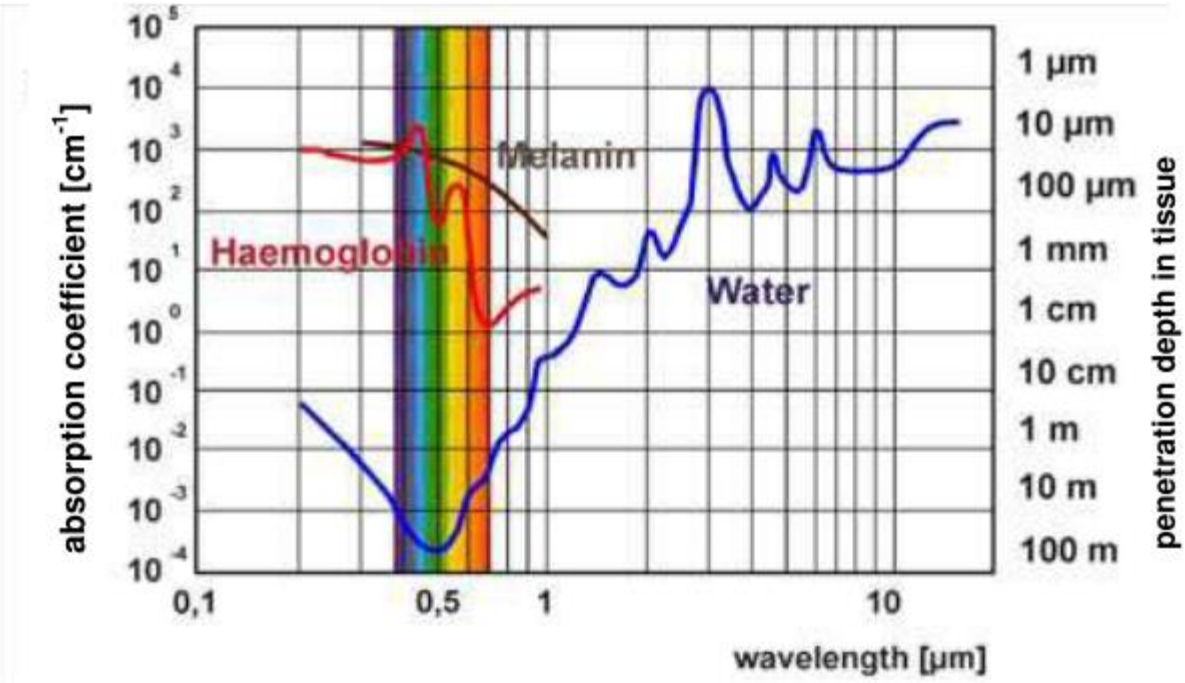

Fig. 1.1: Absorption and penetration depth in water and other biological tissue constituents for different wavelengths [14].

Thulium doped fiber lasers (TDFL) can operate in single longitudinal mode and can be pulsed laser with high peak power. Different groups across the globe have been working on developing 2 µm lasers with a single frequency feature. For example, a single frequency distributed feedback (DFB) thulium doped silica fiber laser operating at 1735 nm was developed in Technical University of Denmark [17]. The length of their laser cavity was about 5 cm, with maximum output power of 59 mW. In 2005, another group developed a MOPA at 1836 nm. [18]. The amplified output was about 345 mW. A linewidth of 3 kHz at 1950 nm was obtained by a 2 cm distributed Bragg reflector (DBR) fiber laser [19]. In another experiment 580 mW at 1943 nm was obtained by using a DBR laser pumped by a single mode fiber laser at 1575 nm. [20]. An

output power of 102 W was also demonstrated by using a Tm^{3+} doped MOPA system at 1970 nm [21].

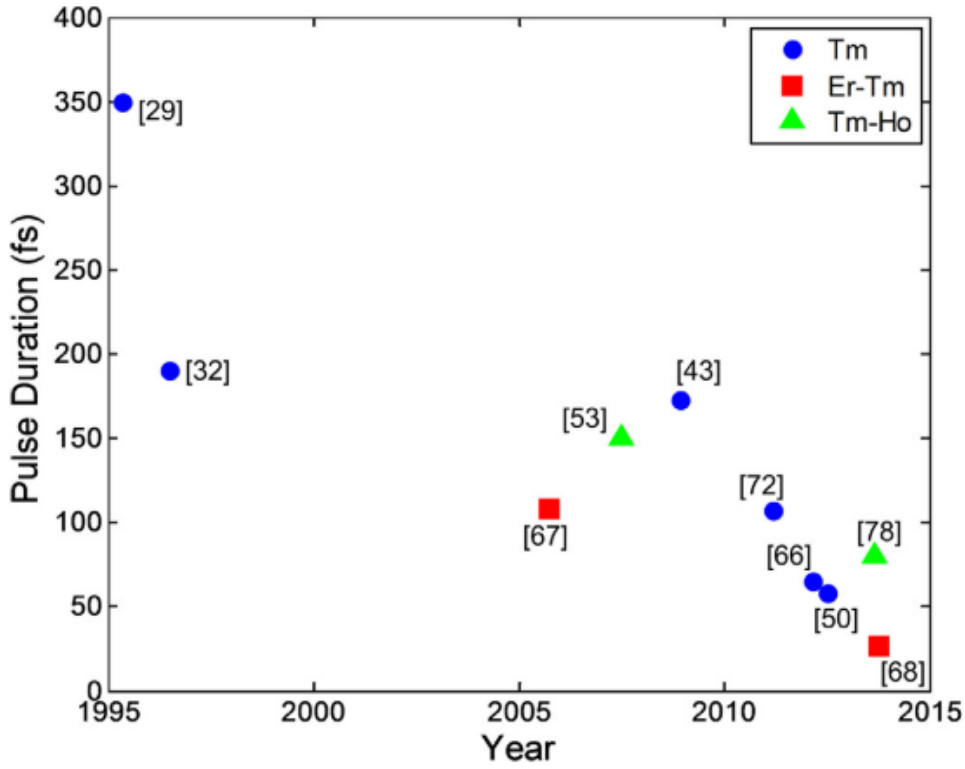

Fig. 1.2: Summary of shortest pulses durations observed over time in mode-locked Tm-doped fiber laser systems [22].

As mentioned above, TDFLs can be operated in the pulsed regime. In 2009, all fiber Q-switched pulsed laser operating at 1950 nm with a wide range of repetition rates was developed. The repetition rate was between tens of hertz to hundreds of kilohertz [23]. There are various demonstrations with different laser power of ns pulse widths in the 2 μm region [24–25]. TDFLs can also be operated in the mode-locked regime in the 2 μm region [26–27]. Fig. 1.2 summarizes shortest pulses durations which were observed in mode-locked Tm-doped fiber laser up until 2014 [22].

1.3 Spectroscopy of thulium doped silica for mid IR emission

The science of interaction of matter with electromagnetic wave is known as spectroscopy science. Spectroscopists study the electronic and physical properties and structure of matter at the atomic scale. The spectroscopy of materials can lead to better understanding of laser slope efficiency, photon absorption, gain, saturation intensity, etc.

As shown Table 1.1 silica glass has interesting properties, such as a very high glass transition temperature [28], that make it favorable as a host for rare earth ion-based fiber lasers.

Table 1.1: Basic properties of silica glass [28].

Glass Property	**Silica**
Transmission range (μm)	0.16-4
Maximum phonon energy(cm^{-1})	1100
Transition temperature (C)	1175
Specific heat (J/(g.K))	0.179
Thermal conductivity (W/(m.K))	1.38
Expansion coefficient (10^{-6}/K)	0.55
Density (g/cm^3)	2.20
Knoop hardness (kg/mm^2)	600
Fracture toughness ($MPam^{1/2}$)	0.72
Poisson's ratio	0.17
Young's modulus (Gpa)	70
Shear's modulus (Gpa)	31.2
Bulk's modulus (Gpa)	36.7
Refractive index (@ 589 nm)	1.458
Abbe number	68
Zero material dispersion wavelength (μm)	1.3
Nonlinear index (10^{-13} esu)	1
Thermo optics coefficient (10^{-6}/K)	11.9

The energy level diagram of Tm^{3+} doped silica for 2 µm region emission is shown in Fig. 1.3. As can be seen $3F_4 \rightarrow {}^3H_6$ can emit between 1700 to 2100 nm with in-band pumping possible from 1550 to 1900 nm. Photons with the wavelength of around 1200 nm can populate ${}^3H_5$ and then due to nonradiative transition the ${}^3F_4$ level will be populated.

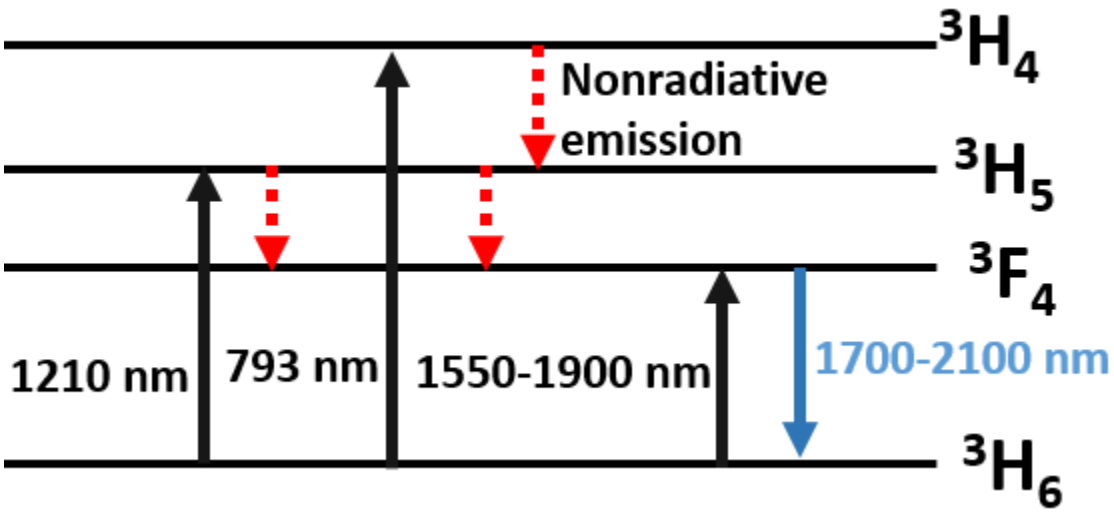

Fig. 1.3: Energy level diagram of Tm^{3+} doped silica for 2 µm region emission.

Fig. 1.4 shows the absorption and emission of thulium doped silica. The highest absorption belongs to ${}^3H_6$ -> ${}^3H_4$; note the absorption into ${}^3H_5$ is stronger than the absorption into ${}^3F_4$.

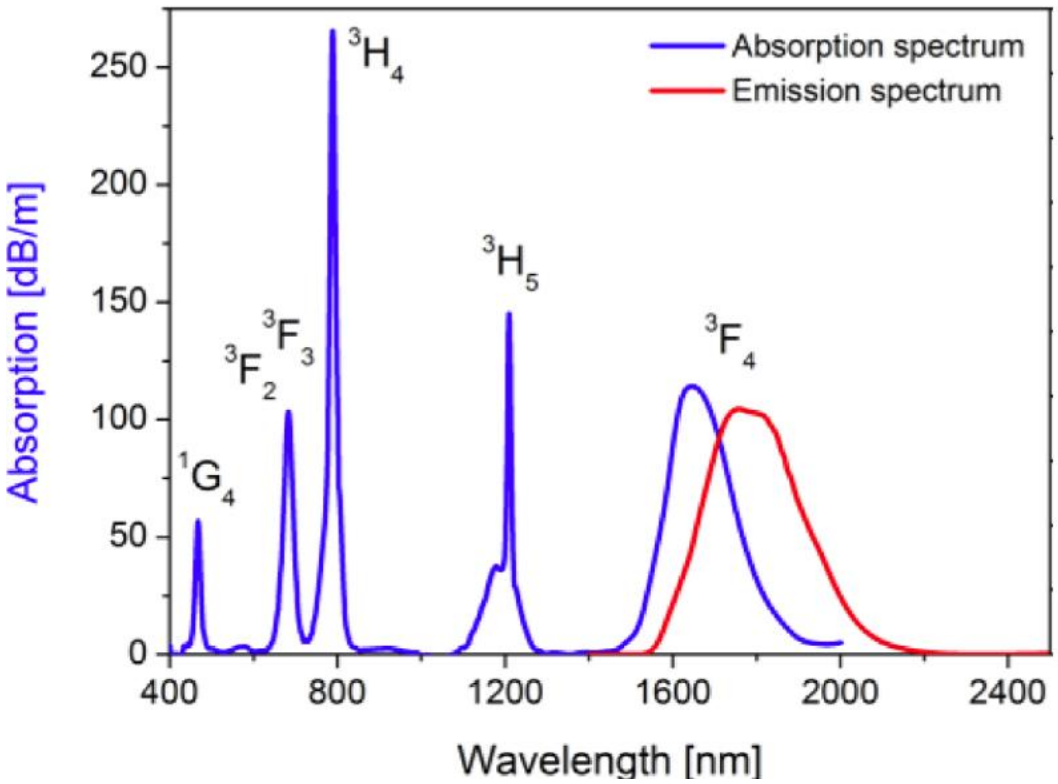

Fig. 1.4: The optical absorption and emission spectra of thulium doped silica fiber [29].

It is usually better to pump the Tm^{3+} doped silica to $^3H_4$ to get $^3F_4 \rightarrow {}^3H_6$ emission, because pump power at 800 nm is readily available and it can also have high quantum efficiency [23], which is due to the cross relaxation as shown in Fig. 1.5. In this process the ion "a" is in some excited state, as a part of its energy is moved to another ion, denoted as ion"initially in the electronic ground state, which results in both ions finally being in the upper laser level at $^3F_4$.

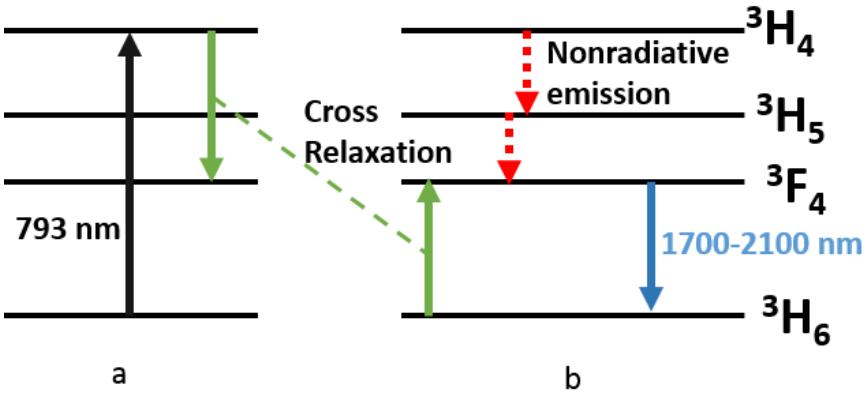

Fig. 1.5: The cross relaxation process between two thulium ions labeled as “a” and “b”.

.

Chapter 2 Fiber Laser Fundamentals

Three fundamental components are needed for all laser systems, namely a gain medium to provide light generation and amplification, a cavity to provide optical feedback, and a pump source to provide population inversion. Fiber lasers are a laser subgroup that rely on cylindrical glass waveguides to confine the pump and laser light near an optically active core. The benefit of this design is the large overlap of the pump light and gain region, as they provide high gain inversion with relatively low pump powers. Other benefits consist of the lack of constant alignment, compact footprints, high beam quality, lower cost to manufacture, and access to unique wavelengths [25].

2.1 Light Amplification by Stimulated Emission of Radiation

2.1.1 Optical cavity

An optical cavity can be comprised of just two mirrors in a Fabry-Perot geometry or it can be a more complicated design. In its simple form the two mirrors can trap the light and photons travel inside of this cavity for a period of time. The reflectivity of the mirror determines the period of time, number of round trips, etc. In the cavity usually one mirror has high reflection (>90%) and the other one should have lower reflection to allow the light to exit the cavity, providing laser output.

2.1.2 Gain media

The gain medium is usually placed between the two mirrors inside of the cavity. For optical pumping, the properties of the gain medium are such that it can optically activated with an electronic structure that can create population inversion. The minimum number of energy levels

that the gain medium must have to lase is three. Usually, these three levels are referred to as the ground level, the excited level and the lasing level. The lifetime of the excited level should be short, and it should immediately decay to the lasing level.

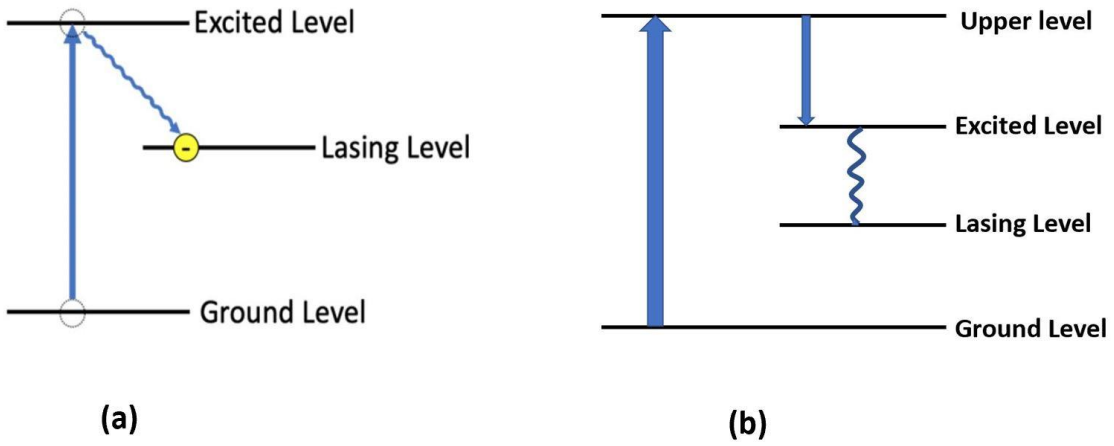

Figure 2.1: Diagram of (a) three level (b) four level laser schemes

On the other hand, the lifetime of the lasing level should be long enough to obtain a population inversion. For laser oscillation, the population inversion must be > 1. which means the ratio of ions in the excited stare to the ground state is greater than one. For a given gain medium at thermal equilibrium, the population inversion can be written as:

$$\frac{N_2}{N_1} = e^{\frac{-(E_2-E_1)}{kT}} \quad (2.1)$$

where E_2 - E_1 is the energy difference between the excited and the ground state, N_2 is the population density of the excited state, N_1 is the population density of the ground state, and k and T are the Boltzmann constant and temperature of the atoms respectively.

2.1.3 Pump source

In order to have population inversion the electrons must go from ground state to excited state, this process needs energy to make the electrons leave the ground state to reside in excited state. For this process a pump source is needed to generate this energy. In fiber laser usually the pump source is a laser but in general the source can be flashlight or electrical pumping. The rate at which energy is absorbed by the ground level is equal to

$$\frac{\partial N_1}{\partial t} = -B_{12}\rho(\lambda_{12})N_1 \quad (2.2)$$

where B_{12} is the proportionality constant and $\rho(\lambda_{12})$ is the radiation energy density. The rate of absorption is also related to the instantaneous photon density, $I_\lambda\,/(hv)$, and the wavelength specific absorption cross-section, σ_λ^a, of the gain media.

$$\frac{\partial N1(t)}{\partial t} = -\sigma_\lambda^a \frac{I\lambda}{(hv)} N_1(t) \quad (2.3)$$

2.1.4 Emission

When the electrons are in the excited state, they can emit energy and go back to the ground state. This event is called emission. The usual and common kind of emission is spontaneous emission where photons are emitted due to random decay of excited electrons. The rate of this decay is described by the Einstein A coefficient, A_{21}, and is inversely proportional to the lifetime of the excited state, τ_{21}.

$$\frac{\partial N_2(t)}{\partial t} = -A_{21}N_2(t) = -\frac{N_2}{\tau_{21}} \quad (2.4)$$

2.1.5 Amplification

If the photons that are produced due to deexcitation of electrons interact with each other and obtain the same phase, they will emit coherently which is referred to stimulated emission. The rate of stimulated emission is given by,

$$\frac{\partial N_2}{\partial_t} = -B_{21}\rho(\lambda_{21})N_2 = -\sigma_\lambda^e \frac{I\lambda}{(h\nu)} N_2 \quad (2.5)$$

where σ_λ^e is the emission cross-section. It is easy to see that since one photon has created two and those two will create more, coherent amplification of the original emitted photon can grow exponentially.

2.1.6 Resonance

For a laser, it is not sufficient to only have stimulated emission. Feedback of the optical signal must also occur. The optical path length of a cavity determines the number of modes and for a cavity of length L, the longitudinal modes are equal to an integer multiple of half the wavelength λ, and the frequency spacing can be shown to be:

$$FSR = \Delta\nu = \frac{c}{2nL} \quad (2.6)$$

2.1.7 Rate equations

The rate equations for a three-level laser system can be written as:

$$\frac{dN_3}{dt} = W_{13}N_1 - \Gamma_{32}N_3 \quad (2.7)$$

$$\frac{dN_2}{dt} = W_{12}N_1 - W_{21}N_2 - \Gamma_{12}N_2 + \Gamma_{32}N_3 \quad (2.8)$$

$$\frac{dN_1}{dt} = -W_{13}N_1 - W_{12}N_1 + W_{21}N_2 - \Gamma_{12}N_2 + \Gamma_{32}N_3 \quad (2.9)$$

where N_1 is the population density of the energy level, Γ_{12} is the inverse lifetime of the energy state transition, and W_{12} is the pump rate of the relevant energy levels.

State $|3\rangle$, has a rapid decay compared to other excited states, so we can have a steady state given by $dN/dt = 0$. The steady state solutions for a three-level system is

$$n_2 = \frac{W_{13}}{W_{13} + W_{21} + \Gamma_{21}} \quad (2.11)$$

$$n_1 = 1 - n_2 \quad (2.12)$$

where n_2 and n_1 are the normalized population densities.

Chapter 3 Fiber laser and fiber amplifier in 2 μm region

3.1 Motivation

As discussed in Chapter 1, 2 μm lasers have many different applications. As examples, they are desirable for light detection and ranging (LIDAR) and sensing systems, as they are more efficient than 1 μm lasers, due to smaller atmospheric scattering and atmospheric distortion. 2 μm lasers are also good options for non-metal material processing applications such as direct cutting, welding, and drilling. Among the rare earth ions doped lasers, thulium and holmium doped lasers can operate in 2 μm region.

3.2 Thulium doped fiber laser operating at 1940 nm

Tm^{3+} doped silica can emit between 1700 to 2100 nm due to the $^3F_4 \rightarrow {}^3H_6$ transition. The $^3F_4$ energy level can be populated by in-band pumping. The wavelength range for in-band pumping can be from 1550 to 1900 nm as shown in Figure 3.1.

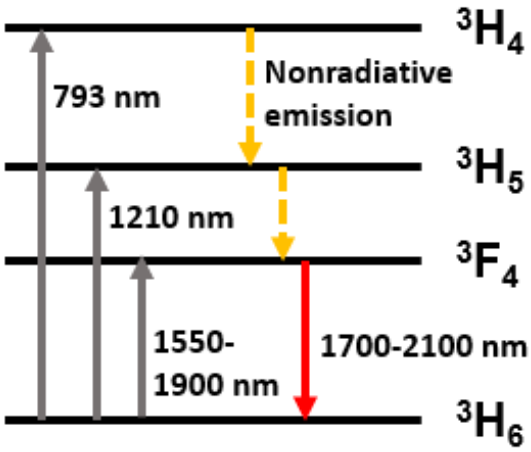

Figure 3.1: Energy level diagram of Tm^{3+} doped silica for 2 μm region emission.

A 1210 nm pump laser can also be used to populate $^3F_4$ energy level, as can a 790 nm pump source with two consecutive nonradiative decays.

3.2.1 790 nm pump source

The highest absorption cross section of Tm^{3+} doped silica is in the 790 nm band which populates the $^3H_4$ energy level. The lifetime of $^3H_4$ is around 20 µs [30]. As shown in Figure 3.1, two nonradiative emissions from $^3H_4$ are needed to populate $^3F_4$. The availability of high pump power around 800 nm and quantum efficiency of greater than 100% are the two main advantages of using this pump source [31]. The high quantum efficiency is due to the cross relaxation as shown. In this process the ion "a" is in $^3H_4$, a part of its energy is transferred to some other ion which in here is ion"b", which is originally in the electronic ground state, and both ions are finally in the upper laser level at $^3F_4$ as shown in Figure 3.2 .

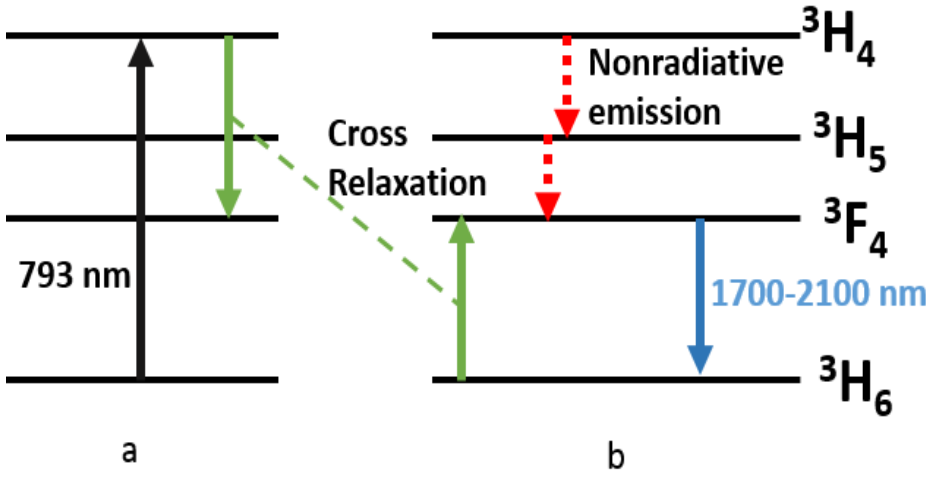

Figure 3.2: The cross relaxation process between two thulium ions labeled as "a" and "b".

Tm^{3+} doped double clad fiber from IX blue was used with 6.5 dB/m absorption at 790 nm. In this experiment a pump diode at 793 was used as the pump source as shown in Figure 3.3. The pumps

diode was installed on a cooling plate which was cooled by a water chiller usin. The combiner had two inputs for pump power where multimode fibers were used, and one signal port input where SMF28 (single mode) fiber was used. The common port was double clad with a core diameter of 10 µm.

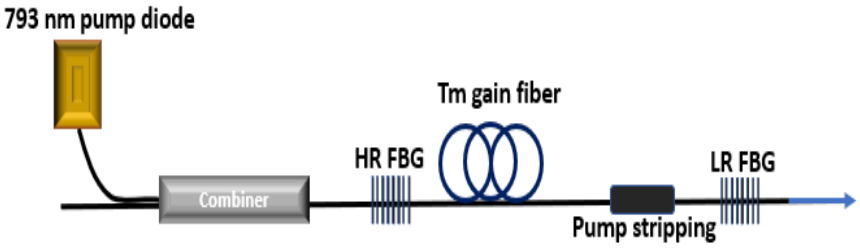

Figure 3.3: Schematic of laser setup operating at 1940 nm.

The high reflection (HR) FBG used double clad fiber at 1940 nm with 1.93 nm reflection bandwidth and 99.9% reflectivity; the low reflection (LR) FBG was also a double clad fiber at 1940 nm with 0.55 nm reflection bandwidth and 9.22% reflectivity. A pump stripper was used to remove all the pump power in the cladding before the LR FBG. Tm^{3+} doped double clad fiber with two different lengths (1.3 m and 2.3 m) was used as the gain fiber. The core diameter of gain fiber was 10 µm with an NA of 0.14, the cladding diameter was 125 µm with an NA of 0.46.

Figure 3.4 shows the output laser power as a function of pump power for 1.3 and 2.3 m. The efficiency of the 1.3 m laser is lower than the 2.3 m laser by 3%. The slope efficiency for the 1.3 m fiber laser was 36% and for the 2.3 m fiber laser was 39%. The pump threshold for the 1.3 m fiber laser was about 1.6 W while that for the 2.3 fiber laser was about 1.9 W. The maximum obtained laser power was 5 W for the 2.3 m fiber laser. Higher pump powers were not used in

either case to ensure that components were not damaged that were needed for further experiments. The spectrum of the laser output is also shown in the inset of Figure 3.4.

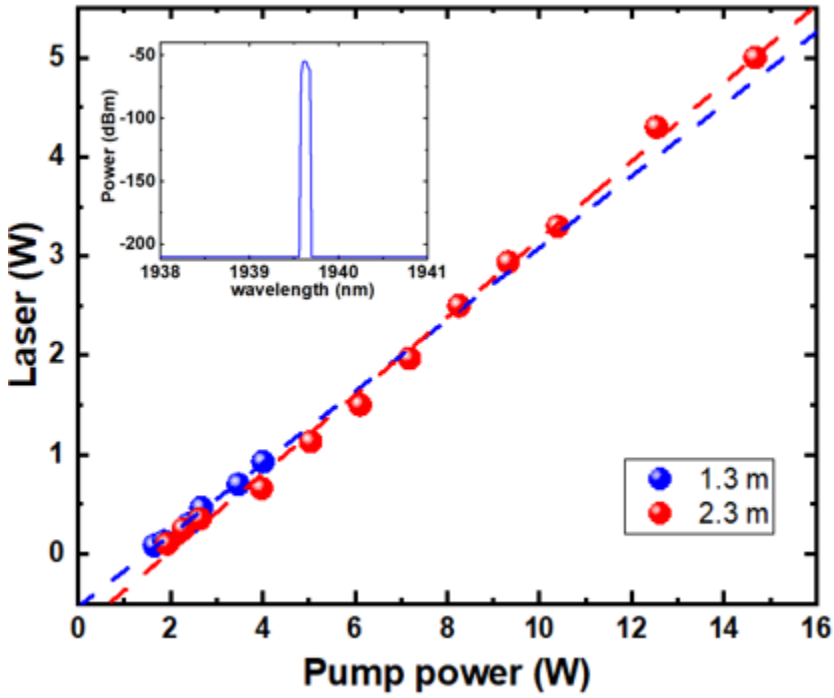

Figure 3.4: Laser output power as a function of input pump power for 1.3m and 2.3 m fiber. Inset: The spectrum of laser output.

Tm^{3+} doped fiber lasers are usually sensitive to the temperature and environment. In this experiment after the 1.3 m fiber laser was operating a fan was applied to the pump stripper and as shown in Figure 3.5 the output power suddenly jumped up significantly. Initially the output power was decreasing with time but when the fan was used, the power jumped up by about 9% which is very noticeable. After applying the fan, the output was monitored for about 20 minutes and no power drop was observed. The power fluctuation was also reduced significantly to about 1% fluctuation.

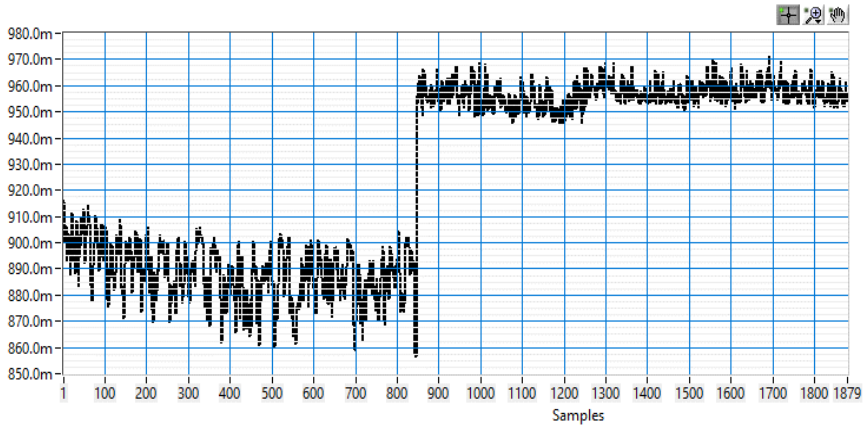

Figure 3.5: Output power of the 1.3 m fiber laser as a function of time.

The built Tm^{3+} doped fiber laser was used as a seed laser for a master oscillator power amplifier (MOPA). The wavelength of the seed laser was 1940 nm and it was amplified by a MOPA. The schematic setup is shown in Figure 3.6. A single-mode fiber laser operating at 1940 nm was used as the seed laser and spliced to an isolator. The isolator was used to make sure that no reflective feedback enters the seed laser, which can damage the laser. The maximum optical power that the isolator could handle was 2 W. The output of the isolator was spliced to the input signal of the combiner which was made of SMF28 fiber. A multimode fiber coupled diode laser operating at 793 nm was used as the pump of the amplifier.

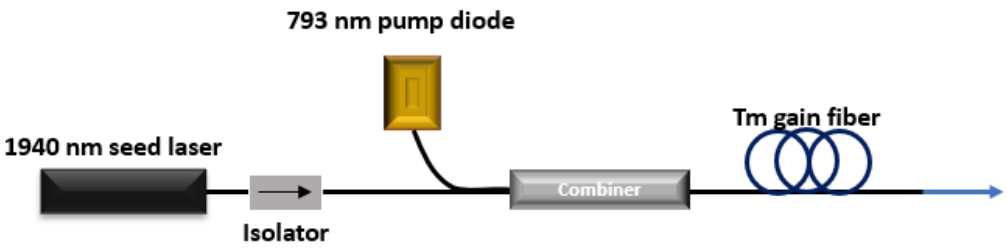

Figure 3.6: Schematic of the MOPA system operating at 1940 nm.

About 5-meter Tm^{3+} doped double clad fiber from IX Blue was used as the gain fiber for the amplifier. The length of the gain fiber for the amplifier was previously optimized for another experiment. The output power was measured as a function of pump power for different input signal powers. Figure 3.7 shows the output power of the amplifier as a function of input pump power for three different input signals power of 0. 42 W, 0.55 W, 0.8 W respectively.

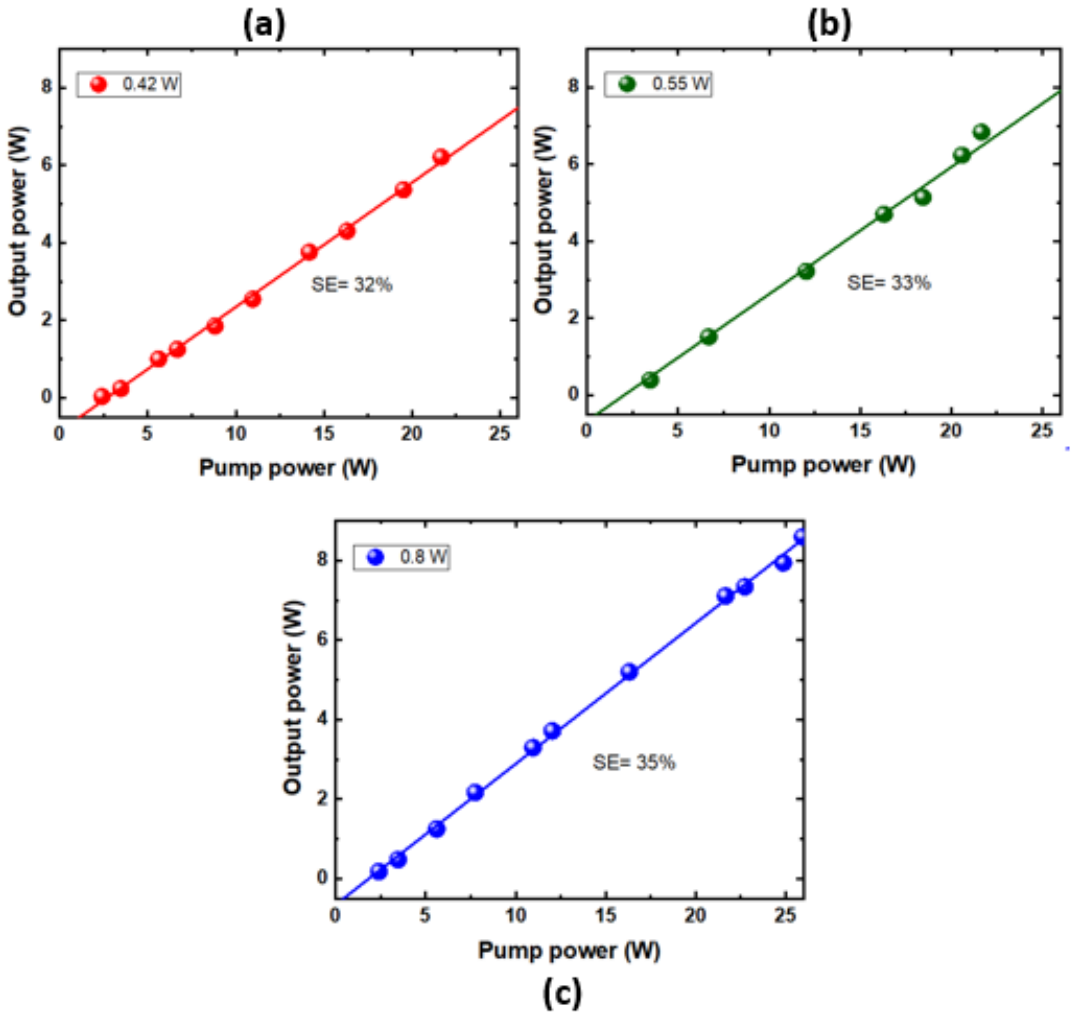

Figure 3.7: The output of the amplifier as a function of pump power for different seed laser input power; (a) 0.42 W; (b) 0.55 W; (c) 0.8 W.

As input signal increases, more of emitted photons contribute to stimulated emission rather than spontaneous emission and so then slope efficiencies of 32%, 33%, and 35% were found for

input signal powers of 0.42 W, 0.55 W, and 0.8W respectively. The threshold pump power of input signal of 0.42 W, 0.55 W, and 0.8W were about 2.6 W, 2.4 W, and 1.8 W respectively.

3.2.2 1210 nm pump source

The second highest absorption cross section of Tm^{3+} doped silica is in 1210 nm band which populates the $^3H_5$ energy level as shown in Figure 3.1. In order to emit in the 2 µm region, a nonradiative transition from $^3H_5$ to $^3F_4$ is needed to populate $^3F_4$.

TH512 core active fiber, a codoped thulium/holmium fiber, was used in this experiment. The nominal absorption at 790 nm is more than 150 dB/m with nominal core NA of 0.16, and cutoff wavelength of 1700 nm. TH512 is a single cladding fiber with a core diameter of 9 µm. the absorption coefficient of TH512 at 1210 nm was found to be about 75 dB/m.

The experimental setup of the fiber laser operating at 1940 nm, using 1210 nm as the pump source is shown in Figure 3.8. The maximum output of the 1210 nm pump diode was about 500 mW with a single spatial mode. A WDM was used to combines the 1210 nm pump laser as the pump, with the 1940 nm signal laser. The TH512 gain fiber was spliced to the common port of the WDM.

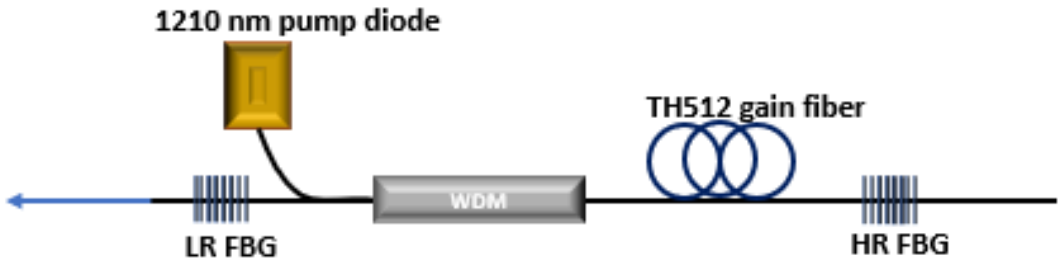

Figure 3.8: Schematic of the laser setup operating at 1940 nm, using 1210 nm pump diode.

The HR FBG was spliced to the gain fiber which was double clad fiber at 1940 nm with 1.93 nm reflection bandwidth and 99.9% reflectivity. The LR FBG was also a double clad fiber at 1940 nm with a 0.55 nm reflection bandwidth, and 9.22% reflectivity was spliced to the signal port. Figure 3.9 shows the output power of; (a) laser signal with 30 cm gain fiber; (b) laser signal with 60 cm gain fiber; (c) residual pump power with 30 cm gain fiber; (d) residual pump power with 60 cm gain fiber, as a function pump power.

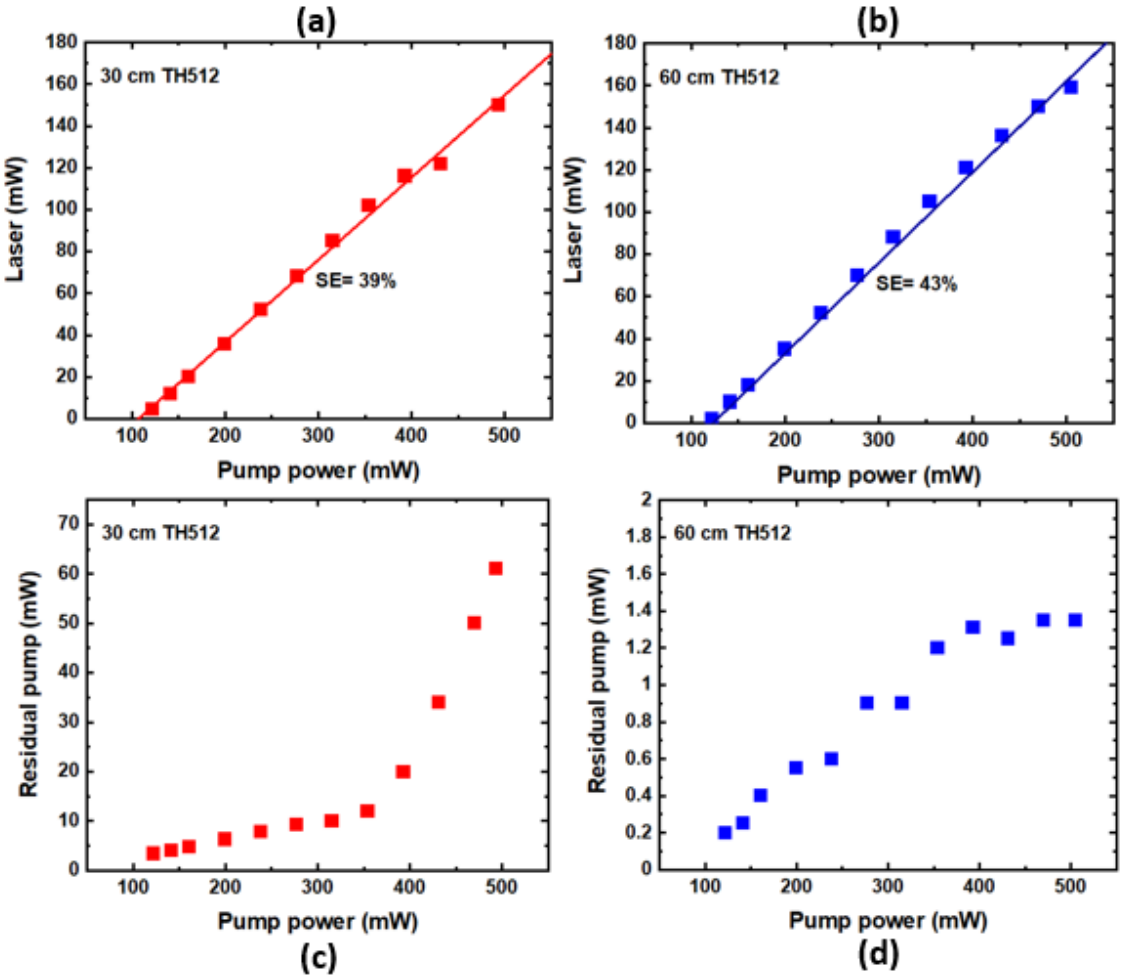

Figure 3.9: The output power of; (a) laser signal with 30 cm gain fiber; (b) laser signal with 60 cm gain fiber; (c) residual pump power with 30 cm gain fiber; (d) residual pump power with 60 cm gain fiber, all as a function pump power.

As it is shown in Figure 3.9, the slope efficiency of the fiber laser with 30 cm TH512 gain fiber was about 39%, and was 43%. for 60 cm TH512 gain fiber The output power of the pump diode was stable, which led to a stable output power laser at 1940 nm. The residual pump power was measured after the HR FBG with a Thorlabs thermal power sensor which usually works better when the power is more than a few mW. The residual pump power of the 60 cm TH512 gain fiber was not significant and the maximum residual pump power was measured to be around 1.4 mW while the input pump power was about 500 mW. The residual pump power of the 30 cm TH512 gain fiber was about 12% of ther input power when the input power was a maximum of about 500 mW. As shown in Figure 3.9 (c) the slope is initially linear till about 400 mW input power and then the slope significantly increased which shows that the depletion of ground state became more significant. The maximum laser output powers for both 30 cm TH512 gain fiber and 60 cm TH512 gain fiber were about 160 mW, but the threshold of pump power was about 108 mW for 30 cm TH512 gain fiber and 124 mW for 60 cm TH512 gain fiber which was expected due to the longer gain fiber. Figure 3.10 shows the spectrum of the laser output at 1940 nm as measured by the Yokogawa optical spectrum analyzer.

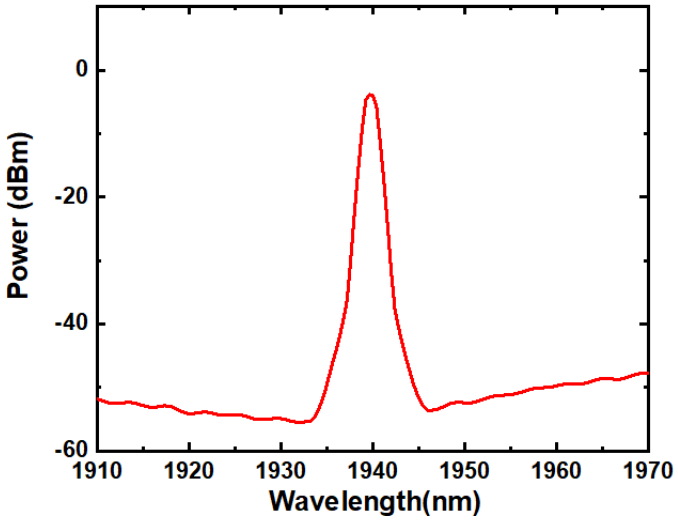

Figure 3.10: The spectrum of output laser operating at 1940 nm.

3.3 Fiber laser operating at 1950 nm

In this experiment, a few watt fiber laser operating at 1950 nm was built. Since a high power fiber-coupled diode pump laser at 793 nm is available, two pump diodes at 793 nm were used as the pump source as shown. Two pump diodes and on combiner were installed on a plate which was cooled by chilled water. The combiner had two inputs for the pump power for which multimode fibers was used, and one input signal port where SMF28 fiber was used. The common port was double clad with a core diameter of 10 µm. As shown in Figure 3.11 Tm^{3+} -doped fiber laser was built to operate at 1950 nm. 3.5 m Tm^{3+} -doped silica fiber with a core diameter of 10 µm was used as the gain fiber. A pair of fiber Bragg gratings (FBGs) were spliced to the gain fiber to form a laser cavity. The FBGs had double claddings, and the output coupler was 40% transmitted. Before the LR FBG, a power stripper was inserted to dump the residual pump power in order to avoid damaging the LR FBG. About 7.5 W of stable output at 1950 nm was obtained, but with increasing pump power the HR FBG was damaged.

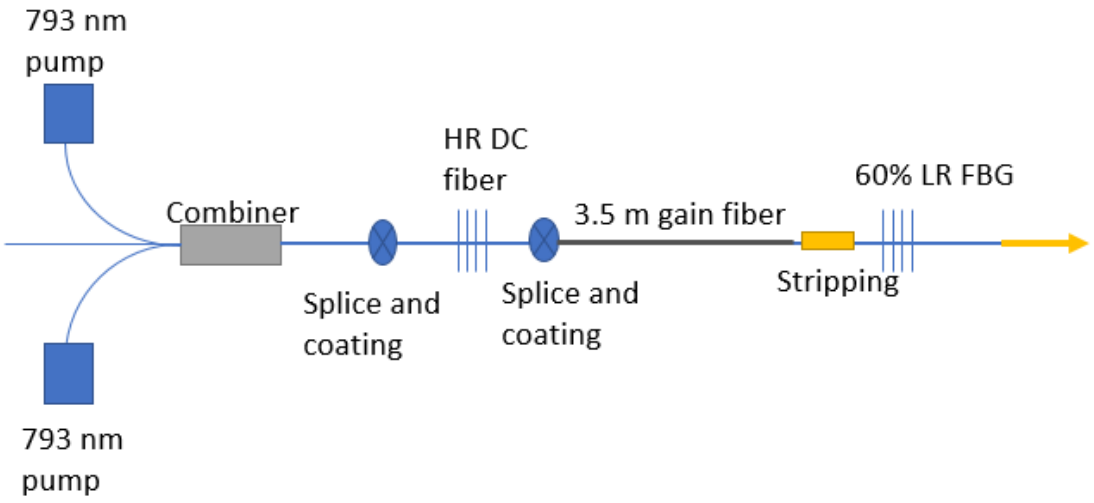

Figure 3.11: A schematic of the laser setup operating at 1950 nm.

Figure 3.12 shows the output power of the laser as a function of pump power. The efficiency of laser is about 37% and the output was stable up to 25 W input pump power. The maximum obtained signal output was 7.5 W. When the pump power increased further the high reflective fiber Bragg grating was damaged. The pump threshold of the laser was about 3 W. The lower right inset of the figure shows the laser spectrum output which is around 1949.5 nm with about 0.1 nm full width half maximum (FWHM). In order to get higher signal output, the high reflective FBG needs a higher quality coating to reduce the power leaking from the outer cladding. Fan cooling the FBG can also help.

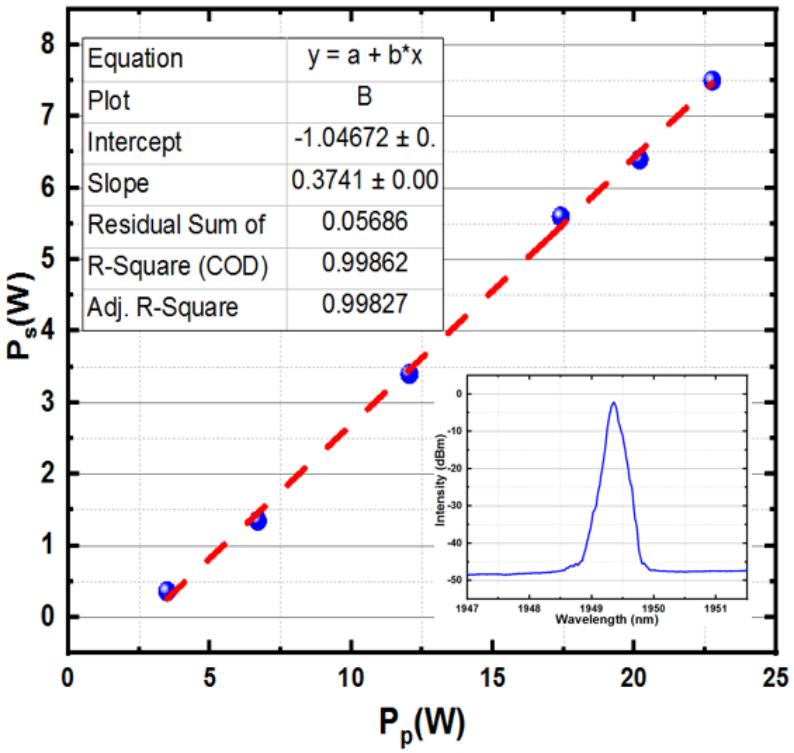

Figure 3.12: The output signal as a function of pump power for 1950nm laseer. Insey: The spectrum of laser output.

3.4 Fiber laser operating at 2050 nm

Although Tm^{3+}-doped silica is able to emit at 2050 nm, its emission cross section is significantly smaller than Ho^{3+}-doped silica. On the other hand, Ho^{3+} absorption is not strong at 793 nm, and 1210 nm. So in many cases Tm^{3+}/Ho^{3+} codoped fibers are used to operate beyond 1950 nm. Figure 3.13 shows the partial energy level diagram of Tm^{3+}/Ho^{3+} codoped silica. Ho^{3+} can be pumped to $^5I_7$ by in-band pumping in the 1900-2000 nm wavelength range. An 1150 nm pump source can also be used to populate $^5I_6$ which can be deexcited to $^5I_7$ by nonradiative emission. Another option is energy transfer from $^3F_4$ of Tm^{3+} to $^5I_7$ of Ho^{3+}. Energy transfer is a phenomena where dopant ions in laser-active media can exchange excitation energy among each other.

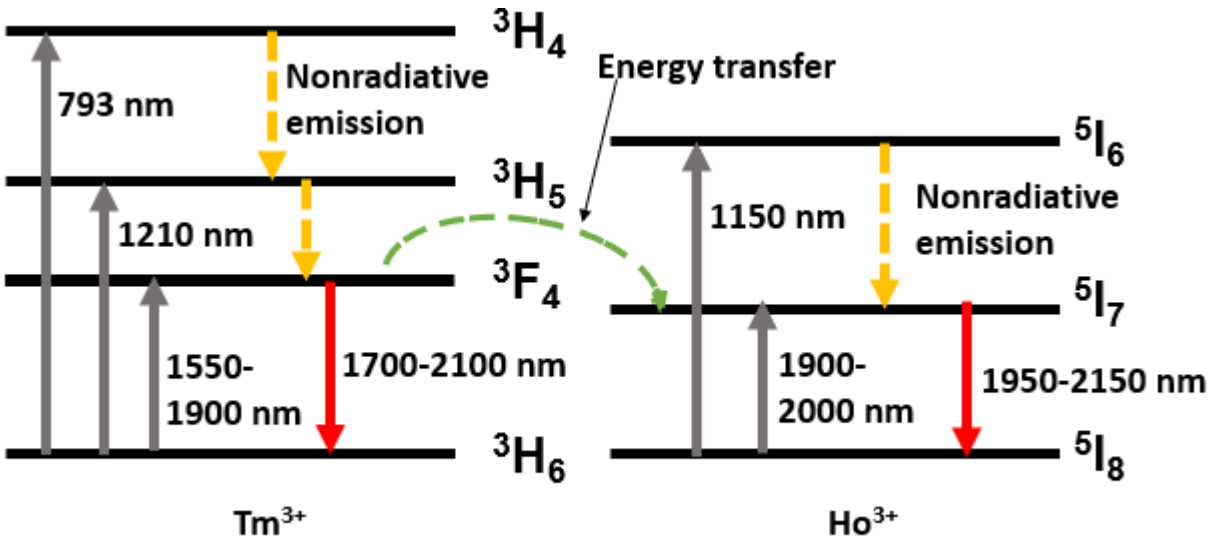

Figure 3.13: Partial energy level diagram of Tm^{3+}/Ho^{3+} co-doped silica.

3.4.1 1940 nm pumping

In order to have high efficiency in band pumping was used to pump Tm^{3+}/Ho^{3+} co-doped silica fiber. The fiber used in this experiment was TH512. 1940 nm laser can be used as a pump to directly pump the ground state of Ho to $^5I_7$.

As shown in Figure 3.14, a 1940 nm fiber laser was used as the pump and a 1950/2050 WDM was used to combine the pump and signal laser. TH512 gain fiber was spliced to the common port of the WDM. The HR FBG was then spliced to the gain fiber. LR FBG was spliced to the signal port of WDM to make sure the output power is just signal laser at 2050 nm. The FBG was SM2000 fiber with a center wavelength at 2049.7 nm. The full width half maximum of LR FBG was 1.8 nm with 94.8% reflection. The full width half maximum of the HR FBG was 1.75 nm with 99.97% reflection.

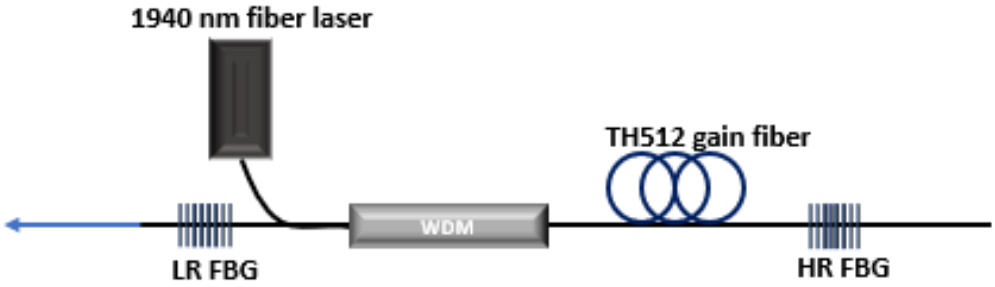

Figure 3.14: Schematic of the laser setup operating at 2050 nm.

In this experiment, 1 m and 2 m TH512 gain fibers were used. Figure 3.15 shows the output power of; (a) laser signal with 1 m gain fiber; (b) laser signal with 2 m gain fiber; (c) residual pump with 1 m gain fiber; (d) residual pump with 2 m gain fiber, as a function of pump power. A Thorlabs Integrating Sphere Photodiode Power Sensor was used to measure the output power of the signal laser and a Thorlabs thermal power meter was used to measure the residual pump

power of the system. The slope efficiency for both fiber lengths were about 3.3%, which is very low, while the slope of the residual pump power is very high. For 1 m gain fiber more than 60% of the 1940 nm pump power wasn't absorbed by TH512 and for 2 m gain fiber more than 50% was not absorbed. This indicates that the Ho^{3+} concentration of TH512 is not large enough to be efficient for lasing beyond 2 µm. The maximum signal laser power was about 25 mW for both 1 m TH512 gain fiber and 2 m TH512 gain fiber.

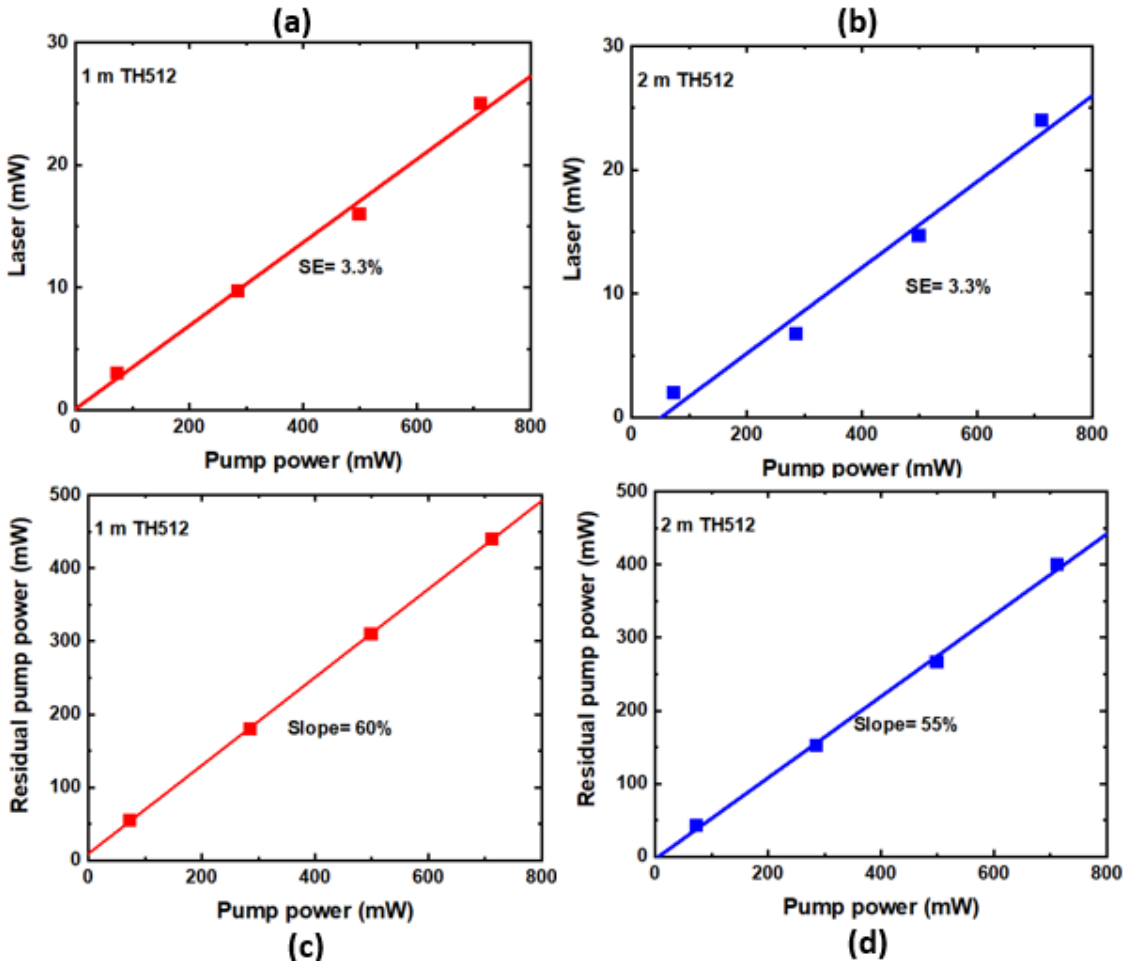

Figure 3.15: The output power of; (a) laser signal with 30 cm gain fiber; (b) laser signal with 60 cm gain fiber; (c) residual pump with 30 cm gain fiber; (d) residual pump with 60 cm gain fiber, as a function pump power.

The spectrum of the laser output is shown in Figure 3.16. The center wavelength is at 2048.98 nm and the full width half maximum was measured to be about 0.1 nm with the resolution of 0.02 nm.

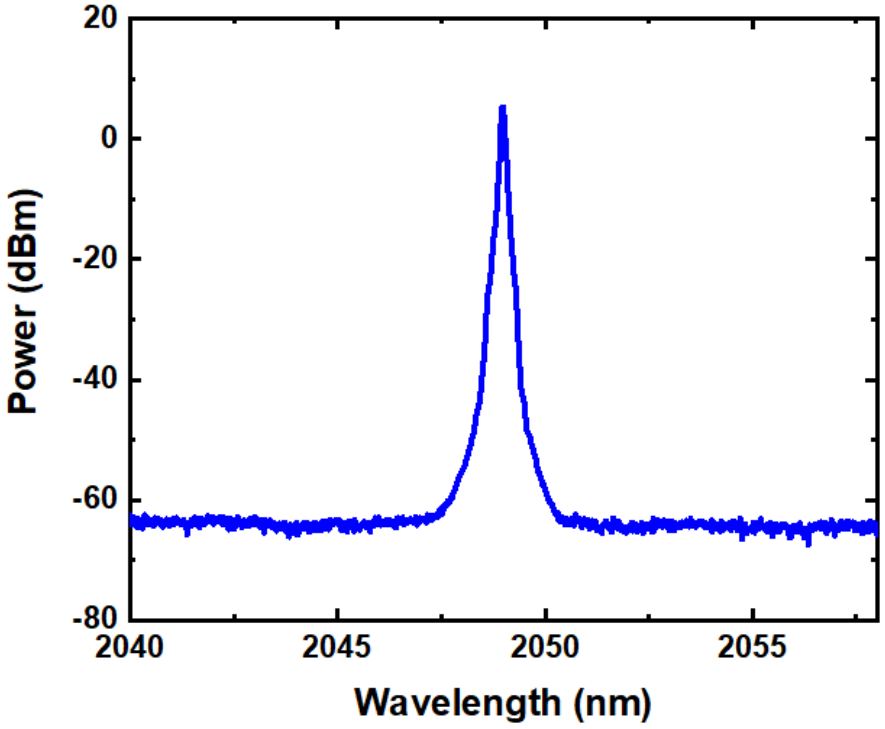

Figure 3.16: The spectrum of laser output operating at 2050 nm.

The amplified spontaneous emission (ASE) of 6.5 m TH512 gain fiber was also measured. The pumping scheme was the same as described above, with a 1940 nm fiber laser used as the pump. Since the absorption of 1940 nm for this fiber is not high, most of the output was 1940 nm even though a WDM was used to separate the 1940 nm pump. The optical spectrum of the ASE is shown in Figure 3.17. The ASE wasn't strong and the emission above 2100 nm is weak.

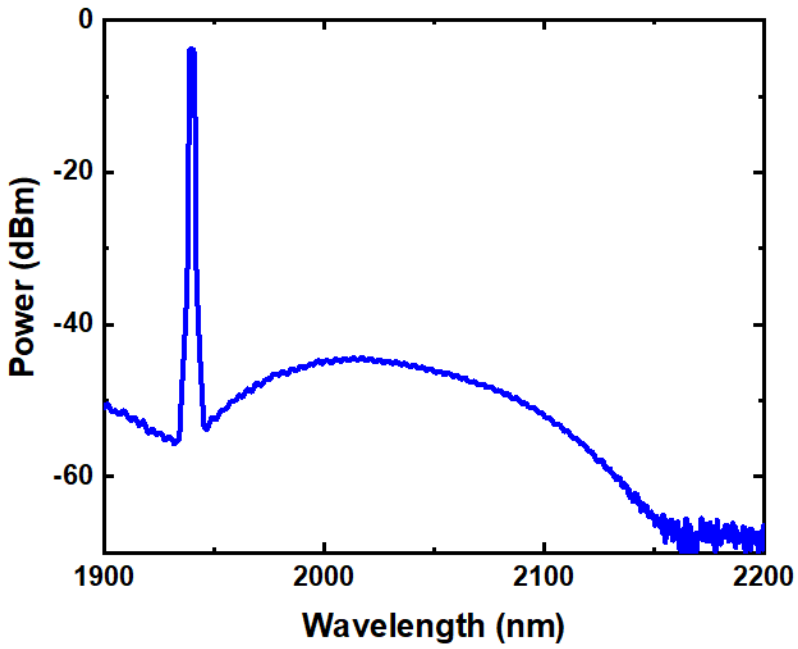

Figure 3.17: The amplified spontaneous emission spectrum of 6.5 m TH512 pumped by 1940 nm laser.

3.4.2 1210 nm pumping

Since the absorption of Ho^{3+} at 1210 nm is low, 1210 nm pumping source is used to raise Tm^{3+} ions to $^3H_5$ and then with the help of nonradiative decay, the $^3F_4$ energy level of Tm^{3+} ions will be populated. Two mechanisms can result in emission at 2050 nm: (1) direct $^3F_4$ to ground state emission can contribute in 2050 nm emission; (2) energy transfer from $^3F_4$ of Tm^{3+} to $^5I_7$ of Ho^{3+} can populate the $^5I_7$ of Ho^{3+} which can emit 2050 nm through the $^5I_7$ to ground state transition. Since the emission cross section of Tm^{3+} is not strong at 2050 nm, we conclude that the main contribution comes from the $^5I_7$ to ground state transition of Ho^{3+}.

In this experiment a 1210 nm laser diode mounted on a Newport diode mount was used which was controlled by a Newport laser driver and temperature controller. Since a 1210/2050 WDM wasn't available in the lab, 1210/1950 WDM was used. The cavity was built with 1 m TH512

and a pair of 2050 nm FBGs. The FBG was SM2000 fiber with acenter wavelength at 2049.7 nm. The full width half maximum of the LR FBG was 1.8 nm with 94.8% reflection. The full width half maximum of the HR FBG was 1.75 nm with 99.97% reflection. In order to monitor and measure the residual pump and also the efficiency of the WDM, two different setups were designed as shown in Figure 3.18. The laser signal output for the setup shown in Figure 3.18 (a) was out of the signal port of WDM and residual pump out of the HR FBG. In the setup shown in Figure 3.18 (b) the LR FBG was both the output of the residual pump and laser signal. The maximum residual pump power measured in the setup shown in Figure 3.18 (a) was about 0.17 mW which is negligible compared to the maximum signal output of 25 mW. This shows that more than 99% of the pump was absorbed.

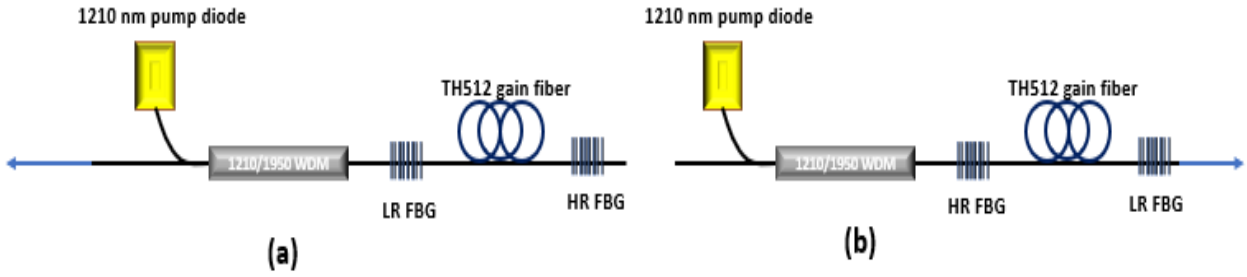

Figure 3.18: Schematic of 1210nm pumped laser setup operating at 2050 nm, (a) signal output from signal port of WDM; (b) signal output from LR FBG fiber.

The maximum output signal for setup shown in Figure 3.18 (a) was about 25 mW and for the setup shown in Figure 3.18 (b) was measured to be about 27.5 mW. This simply shows that even though the WDM wasn't designed for 2050 nm signal it still has a good coupling efficiency. The output power of laser signal as a function of pump power for both setups were measured as shown in Figure 3.19. The pump thresholds for both setups are almost same, ~ 60 mW. The slope efficiencies for both setups are low due to the fact that the $^5I_7$ energy level is not highly populated,

and the number density of Ho^{3+} ions is low. As shown in Figure 3.19 (a) the slope efficiency for the laser setup shown in Figure 3.18 (a) is 6%. Figure 3.19 (b) shows the slope efficiency of another laser setup to be 6.5%. As shown there is a drop in laser output for the laser setup shown in Figure 3.18 (a), which can be due to the fact that as the WDM transmits more pump power the coupling efficiency decreases. In this case the coupling efficiency of the WDM decreased from more than 92% to about 90% for the 2050 nm laser signal.

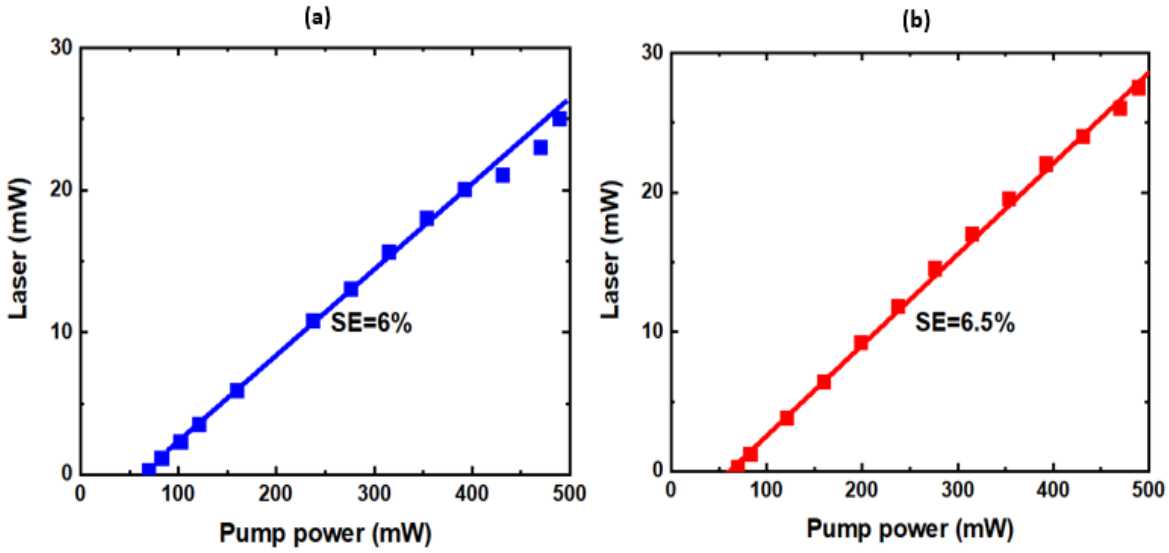

Figure 3.19: The output power of laser signal for (a) laser setup shown in Figure 3.18 (a); (b) laser setup shown in Figure 3.18 (b).

In another experiment, a bidirectional pumping scheme was used as shown in Figure 3.20. Two 1210 nm pump diodes were used to pump 1 m TH512 from both sides. Both pump diodes were spliced to two 1210/1950 WDMs in order to pump the gain fiber. Gain fiber was spliced between a pair of FBGs with center wavelengths of 2050 nm. In the previous experiment, it was shown that the coupling efficiency of 1210/1950 WDM for 2050 nm light is more than 90%.

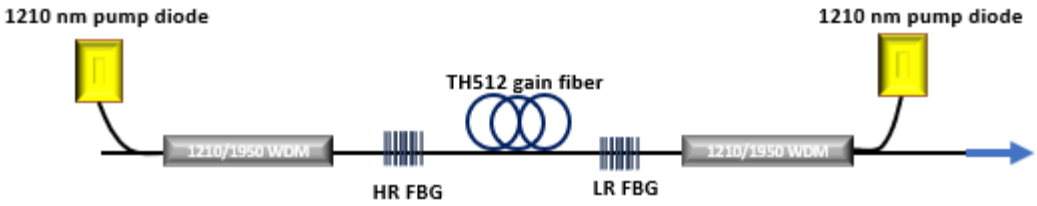

Figure 3.20: Schematic of the laser setup using bidirectional pumping.

Since two pump diodes were used the maximum pump power can go up to about 950 mW. As shown in Figure 3.21, the maximum output laser power is about 55 mW with a slope efficiency of 5.8%. As the gain fiber was pumped harder around 500 mW, the signal started fluctuating, which can be due to the fact that each pump diode was feeding back to the other diode; nevertheless the slope was same as for the one pump diode scheme.

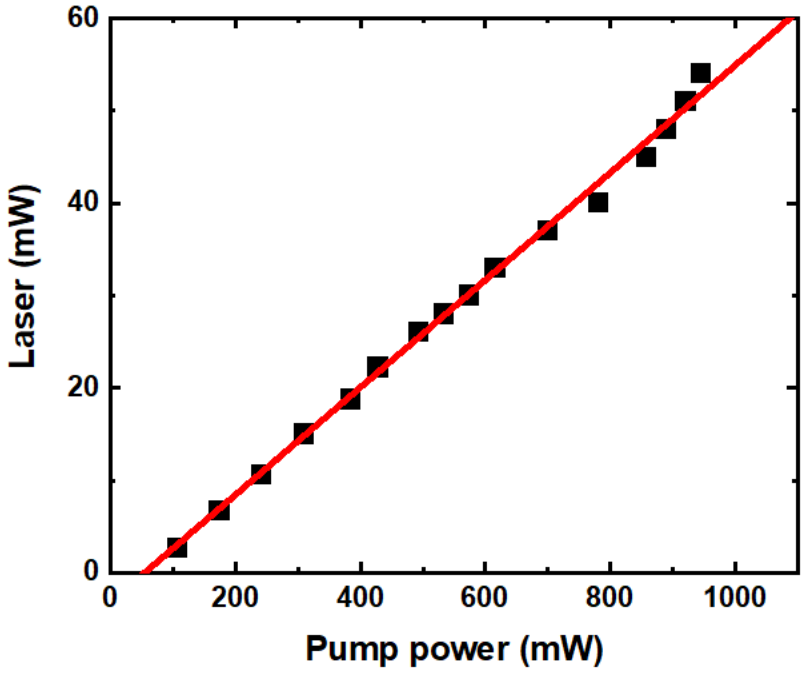

Figure 3.21: The signal laser output power vs. pump power for bidirectional pumping.

In another experiment three different gain fiber lengths of 100, 50, and 25 cm were tested using the same setup as shown in Figure 3.18 (a).

The maximum output powers for the 100, 50, and 25 cm gain fibers were about 25, 15.7, and 15.2 mW, respectively, as shown in Figure 3.22. The slope efficiencies for the 100, 50, and 25 cm gain fibers were about 5.9%, 3.9%, and 3.7%, respectively, thus the slope efficiency of the 100 cm gain fiber is about 1.5 times greater than that of the 25 cm gain fiber. Another interesting point is that the threshold pump power for the 100 cm gain fiber was less than for the other two gain fibers.

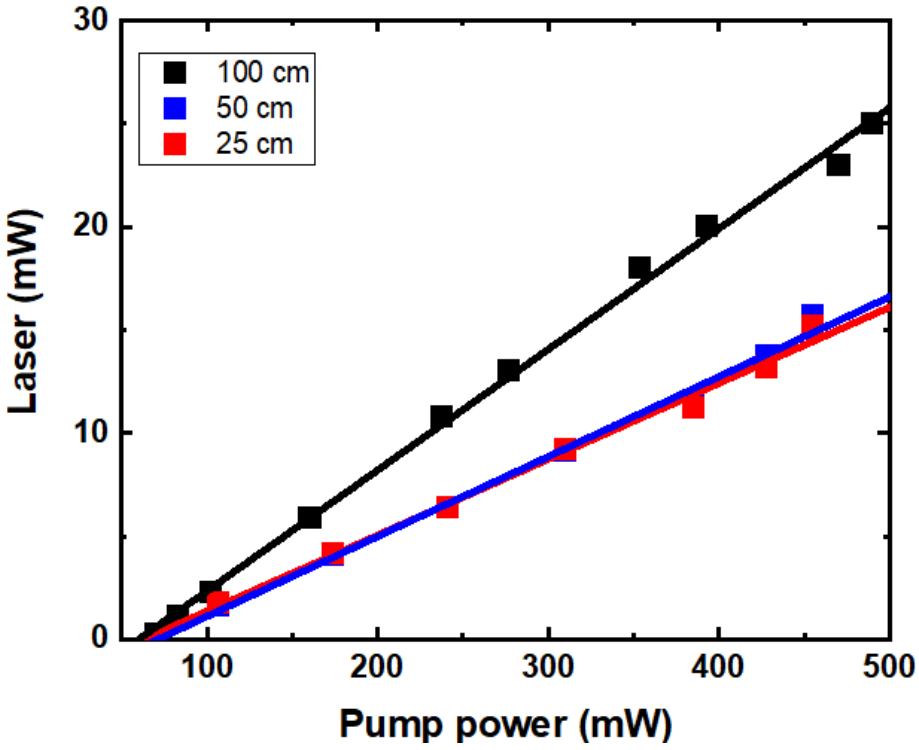

Figure 3.22: Laser output vs pump power for gain fibers with lengths of 100, 50, and 25 cm.

3.5 Q-switched laser and Pulsed laser operating at 1940 nm

In order to generate nanosecond to microsecond pulses with high energy and high peak power, Q-switched lasers are usually used. In this section, two different designs for active Q-switched lasers that were built will be introduced: linear cavity design and ring cavity design. The designs are grounded on active Q-switching, with the help of an acousto-optic modulator (AOM).

3.5.1 Q-switched Ring cavity laser

The ring cavity setup is shown in Figure 3.23 for 793 nm pumping. In order to pump the 1.6 m double clad gain fiber, a diode pump was used; a pump stripper was applied to dump the residual pump in order to protect the AOM. The maximum input average power for the AOM was 150 mW. Once the residual pump was removed, a 50/50 coupler operating at 1940 nm was used as the output coupler. At a pump power of 2.9 W, the pulse width was 500 ns; the average power as a function of repetition rate was measured as shown in Figure 3.24.

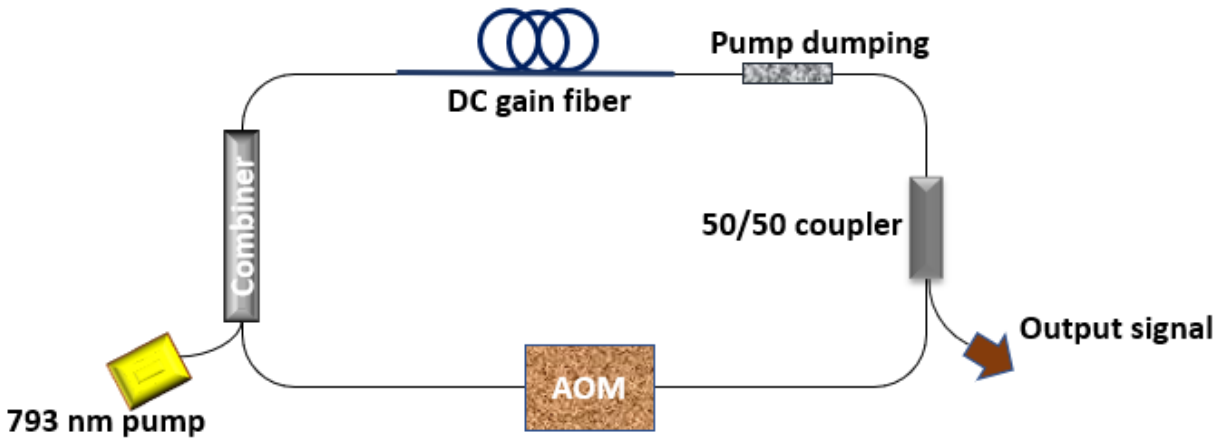

Figure 3.23: Schematic of the Q-switched ring laser cavity design.

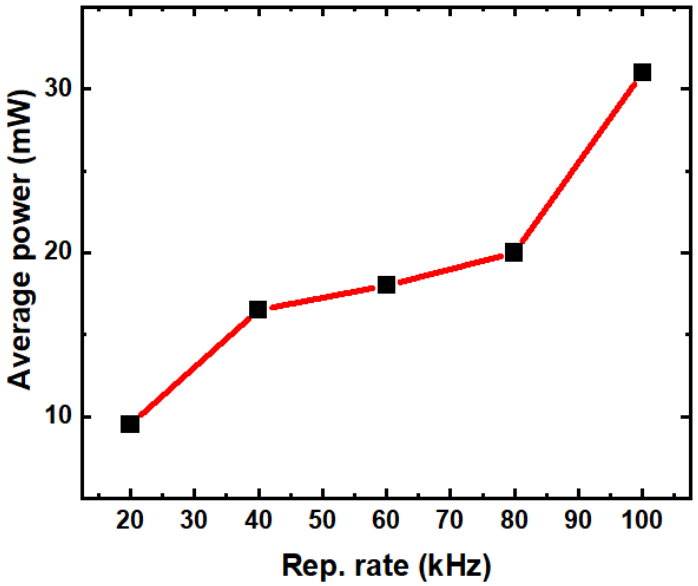

Figure 3.24: Average power vs. repetition rate for a ring laser cavity using double clad fiber and a 793 nm pump diode.

In another experiment, a single clad fiber was used with the length of 80 cm for another test of ring cavity using a 1210 nm laser diode as the pump source.

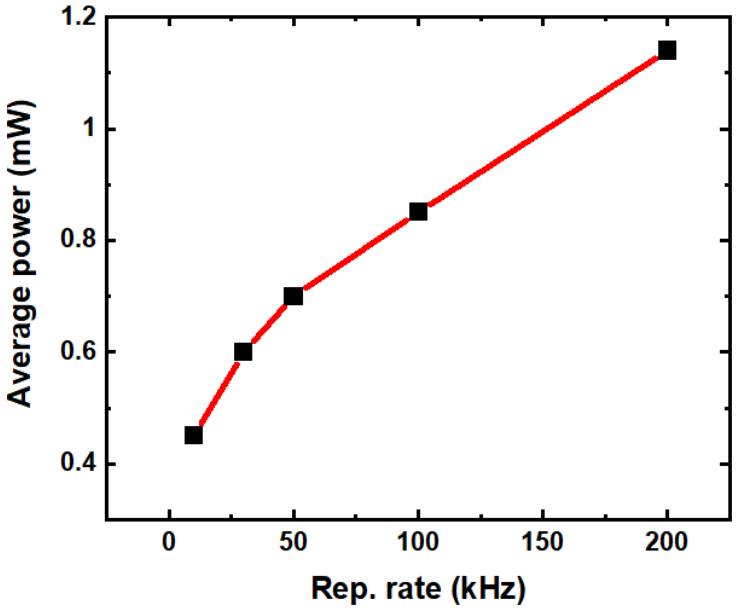

Figure 3.25: Average power vs. repetition rate for a ring laser cavity using single clad fiber and 1210 nm pump diode.

As shown in Figure 3.25, the average output power versus repetition rate at pulse duration of 500 ns was measured for a pump power of about 460 mW. The maximum average power was about 1.2 mW for a 100 kHz repetition rate.

3.5.2 Pulsed laser

The linear cavity design was also tested in this experiment. An average of 80 cm long single clad Tm^{3+}-doped fiber was implemented as the gain medium with a pump diode laser source operating at 1210 nm. A CW laser was built initially to ensure basic operation as shown in Figure 3.26 (a). The output power, as a function of pump power, was tested and a maximum laser power of about 165 mW was achieved with a slope efficiency of 41% as shown in Figure 3.26 (c). However, when an AOM was inserted into the cavity the loss was significant, and no output power was observed, as shown in Figure 3.26 (b).

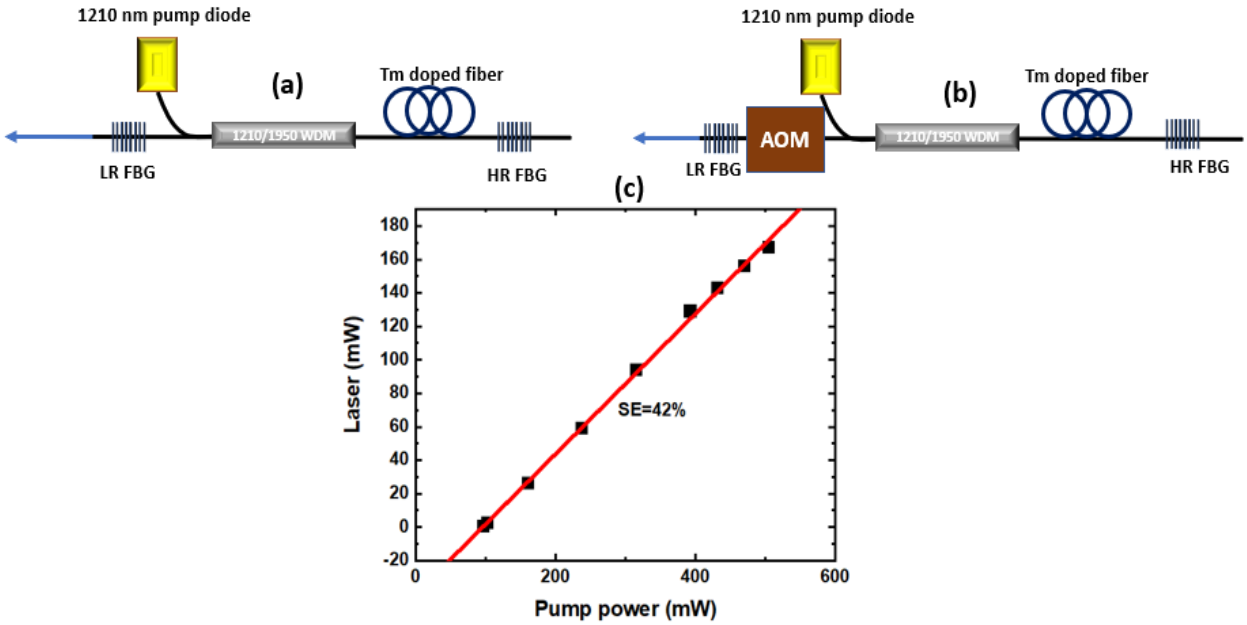

Figure 3.26: (a) CW laser setup linear cavity; (b) Q-Switched laser setup linear cavity; (c) the laser output as a function of pump power for CW laser setup

Since AOM which was inside of cavity didn't work, AOM was placed outside of cavity as shown in Figure 3.27. Note that in this configuration there is no possibility of Q-switching; the AOM is simply being used to make pulses from the CW output.

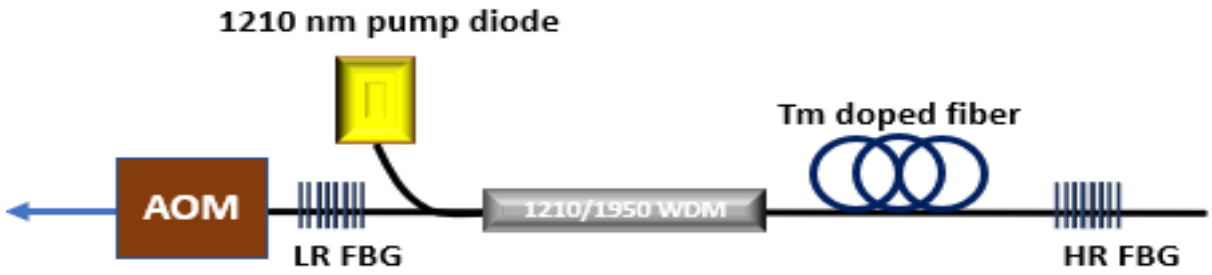

Figure 3.27: Pulsed laser using CW linear cavity and placing AOM outside of cavity.

The table below shows the average output power in µw for different pulse durations and repetition rates with a pump power of about 460 mW.

f(kHz) / t(ns)	**1**	**5**	**10**	**20**	**50**	**100**
50	20	21	23	27.6	40	60
100	20.5	24	28	37	63	107
200	21.3	28.5	37.6	55.7	112	205
500	24	42	66	111	248	484
1000	29	65	110	202	478	949

Table 3-1: Average iutput power in µW for different pulse durations and repetition rate.

In this research he linear cavity setup was also tested. The AOM was spliced to the signal port of the combiner in the linear cavity setup. The schematic design of linear cavity is shown in (a). The pair of FBGs were working at 1940 nm. The HR FBG was applied after the gained fiber and PR FBG were spliced to the output of AOM. The gain fiber was the same as the one used in ring cavity design. (b) shows the average signal power as a function of pump power for the repetition rate of 15 kHz and the pulse width of 50 µs. a signal output power of 10 mW corresponding to 0.66 µJ was attained.

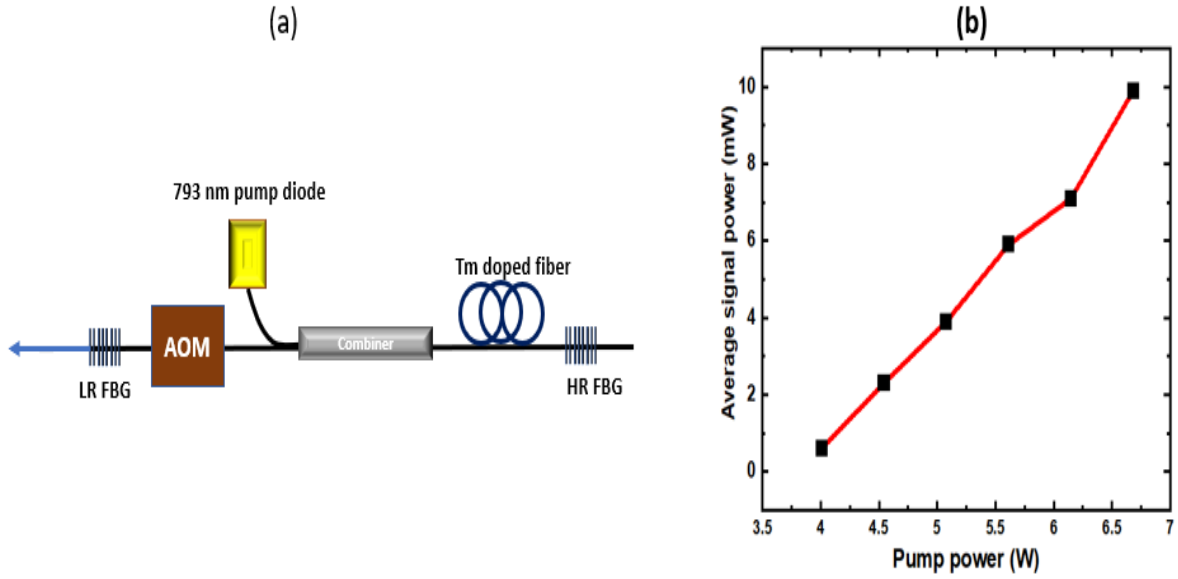

Figure 3.28:(a) The schematic setup of linear cavity design for Q-switched laser;(b) the average signal output power as a function of pump power.

The output of linear cavity Q-switched laser was amplified with one stage amplifier which resulted in a maximum of a few µJ being obtained. Figure 3.29 shows pulse width and repetition rate of the output signal. The pulse duration was about 10 µs with the repetition rate of 10 kHz.

In order to measure the pulse width and repetition rate of the signal a biased free space InGaAs detector was used.

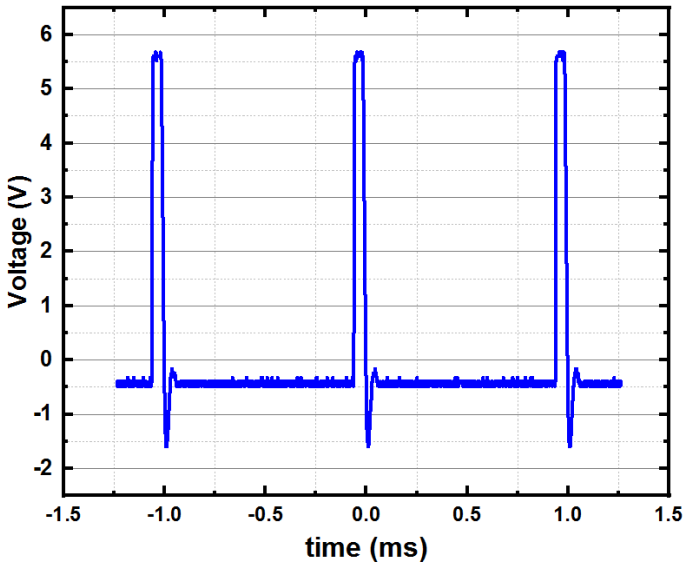

Figure 3.29: The pulse width and repetition rate of output signal.

For 20 kHz and 6.7 W pump using Q-switched laser and then amplify it. And 460 mW for pumping the amplifier the average output power as a function of pulse width was measured. The setup is shown in Figure 3.30.

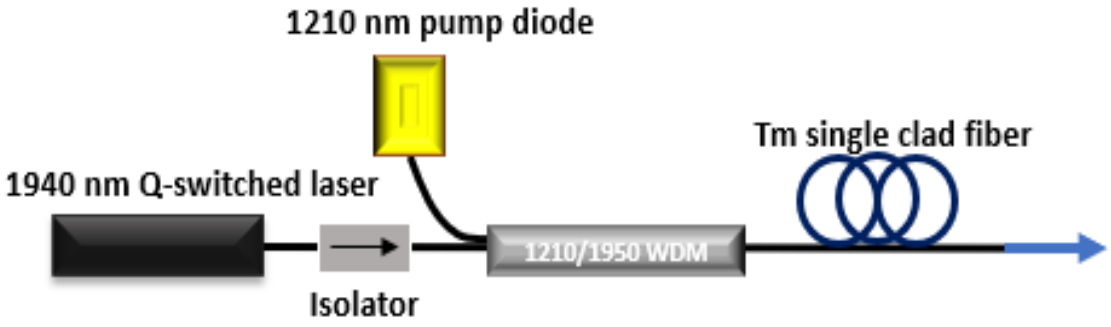

Figure 3.30: The schematic setup of Q swithced laser amplifier

The average signal power as a function of pulse width is shown in Figure 3.31. The maximum output power was about 50 mW with the pulse width of 45 μs.

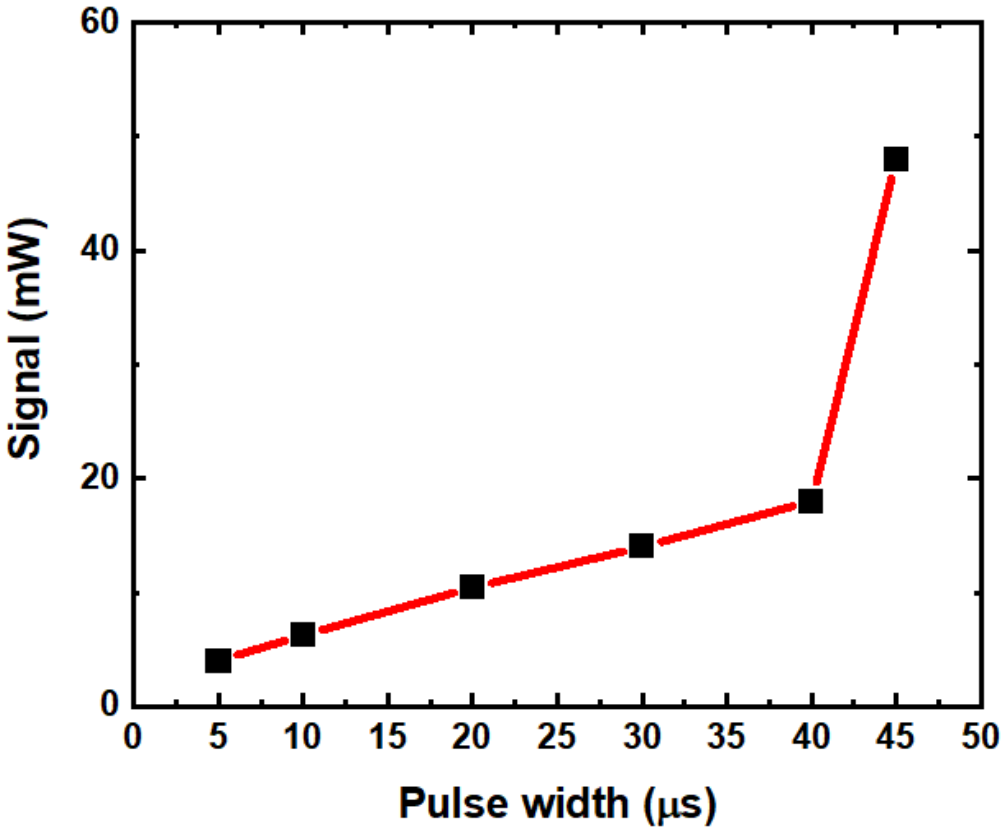

Figure 3.31: Average power as a function of pulsewidth.

Conclusion

In this research the history and theory of the fiber lasers together with the results of multiple experiments on fiber lasers with wavelength in the 2μm region was presented. The Thulium doped fiber laser operating at 1940 nm using a 790 nm pump source and a 1210 nm pump source was investigated. In the case of 790 nm pump source Tm^{3+} doped double clad fiber with two different lengths (1.3 m and 2.3 m) was used as the gain fiber. Based on the experimental setup the efficiency of the 1.3 m laser was lower than the 2.3 m laser by 3% which was expected as 2.3 m laser wasn't fully pumped and reabsorption also was observed. It should be mentioned that the pump threshold for the 1.3 m fiber laser was about 1.6 W while that for the 2.3m fiber laser was about 1.9 W and the maximum obtained laser power was 5 W for the 2.3 m fiber laser. Tm^{3+} doped fiber laser was used as a seed laser for a master oscillator power amplifier (MOPA). The wavelength of the seed laser was 1940 nm and it was amplified by a MOPA. The length of gain fiber was 5-meter Tm^{3+} doped double clad fiber from IX Blue. Different input signal power was demonstrated and the slope efficiencies of 32%, 33%, and 35% were found for input signal powers of 0.42 W, 0.55 W, and 0.8W respectively. In the case of 1210 nm pump source, TH512 core active fiber, a codoped thulium/holmium fiber, was used and the absorption coefficient of TH512 at 1210 nm was found to be about 75 dB/m and the maximum output of the 1210 nm pump diode was about 500 mW with a single spatial mode and the slope efficiency of the fiber laser with 30 cm TH512 gain fiber was about 39% and was 43% for 60 cm TH512 gain fiber.

A fiber laser operating at 1950 nm was also built using coupled diode pump laser at 793 nm. 3.5 m Tm^{3+}-doped silica fiber with a core diameter of 10 m was used as the gain fiber. The efficiency

of laser was about 37% and the output was stable up to 25 W input pump power. The maximum obtained signal output was 7.5 W.

Using codoped Tm^{3+}/Ho^{3+} to build a fiber laser operating at 2050 nm with two different pump source 1940 nm and 1210 nm. In the case of 1940 nm a 1950/2050 WDM was used to combine the pump and signal laser. 1m and 2m TH512 gain fiber was spliced to the common port of the WDM. the slope efficiency for both fiber lengths were about 3.3%, while the slope of the residual pump power is very high. Also, for 1 m gain fiber more than 60% of the 1940 nm pump power wasn't absorbed by TH512 and for 2 m gain fiber more than 50% was not absorbed. This indicates that the Ho^{3+} concentration of TH512 is not large enough to be efficient for lasing beyond 2 μm. The maximum signal laser power was about 25 mW for both 1 m TH512 gain fiber and 2 m TH512 gain fiber. It is also worth to mention that center wavelength as at 2048.98.

An active Q-switched laser was also built. Two setups of ring cavity and linear cavity were investigated both operating at 1940 nm. The ring cavity setup was pumped by 793 nm diode laser and the length o the gain fiber was 1.6 m double clad gain fiber. Using a pump power of 2.9 W, with the pulse width of 500 ns; the average power as a function of repetition rate was investigated. For the linear cavity, an average of 80 cm long single clad Tm3+-doped fiber was used as the gain medium with a pump diode laser source operating at 1210 nm. Different repition rate with different pulse width were investigated. In the laser experiment, the output of linear cavity Q-switched laser was amplified with one stage amplifier which resulted in a maximum of a few μJ output laser withe pulse duration of 10 μs with the repetition rate of 10 kHz.

References

[1] Einstein, A (1917). "Zur Quantentheorie der Strahlung". Physikalische Zeitschrift. **18**: 121–128. Bibcode:1917PhyZ...18..121E

[2] Steen, W.M. "Laser Materials Processing", 2nd Ed. 1998.

[3] Batani, Dimitri (2004). "Il rischio da laser: cosa è e come affrontarlo; analisi di un problema non così lontano da noi" [The risk from laser: what it is and what it is like facing it; analysis of a problem which is thus not far away from us]. wwwold.unimib.it. Programma Corso di Formazione Obbligatorio (in Italian). University of Milano-Bicocca. p. 12. Archived from the original (Powerpoint) on June 14, 2007. Retrieved January 1, 2007.

[4] The Nobel Prize in Physics 1966 Presentation Speech by Professor Ivar Waller. Retrieved January 1, 2007.

[5] "Guide to Lasers". Hobarts. Retrieved April 24, 2017.

[6] Gould, R. Gordon (1959). "The LASER, Light Amplification by Stimulated Emission of Radiation". In Franken, P.A.; Sands R.H. (eds.). The Ann Arbor Conference on Optical Pumping, the University of Michigan, 15 June through 18 June 1959. p. 128. OCLC 02460155.

[7]Chu, Steven; Townes, Charles (2003)."Arthur Schawlow". In Edward P. Lazear (ed.). Biographical Memoirs. **83**.National Academy of Sciences. p.202.ISBN 978-0-309-08699-8.

[8] Joan Lisa Bromberg, The Laser in America, 1950–1970 (1991), pp. 74–77 online

[9] Maiman , T. H. (1960). "Stimulated optical radiation in ruby". Nature. **187** (4736): 493–494. Bibcode:1960Natur.187..493M. doi:10.1038/187493a0. S2CID 4224209.

[10] Townes , Charles Hard. "The first laser". University of Chicago. Retrieved May 15, 2008.

[11] Johnson L. F. Geusic J. E. Uitert L. G. V. 1965 Coherent oscillations from Tm^{3+}, Ho^{3+}, Yb^{3+} and Er^{3+} ions in yttrium aluminum garnet, Appl. Phys. Letters, **7** (5), 127

[12] Caird J. A. De Shazer L. G. Nella J. 1975 Characteristics of room-temperature 2.3-μm laser emission from Tm^{3+} in YAG and $YALO_3$. IEEE J. Quantum Electron., 11

[13] X. Wang, X. Jin, P. Zhou, X. Wang, H. Xiao, Z. Liu, Z. Li, A. M. Heidt, P. S. Teh, M. Berendt, J. K. Sahu, R. Phelan, B. Kelly, S. U. Alam, and D. J. Richardson, "105 W ultra-narroband nanosecond pulsed laser at 2 um based on monolithic Tm-doped fiber MOPA," Opt. Express **23**, 4233–4241 (2015).

[14] K. Scholle, S. Lamrini, P. Koopmann, and P. Fuhrberg, Frontiers in Guided Wave Optics and Optoelectronics (2010).

[15] D. Kracht, H. Sayinc, S. Yilmaz, M. Wysmolek, K. Hausmann, C. Ottenhues, D. Wandt, A. Wienke, and J. Neumann, "Innovative laser sources operating around 2 μm," Phys. Procedia **83**, 1184–1195 (2016).

[16] N. Leindecker, A. Marandi, R. L. Byer, K. L. Vodopyanov, J. Jiang, I. Hartl, M.

[17] S. Agger and J. H. Povlsen, "Single-frequency thulium-doped distributed-feedback fiber laser," Opt. Lett. **29**, 1503–1505 (2004).

[18] N. Y. Voo, J. K. Sahu, and M. Ibsen, "345-mW 1836-nm single-frequency DFB fiber laser MOPA," IEEE Photonics Technol. Lett. **17**, 2550–2552 (2005).

[19] J. Geng, Q. Wang, T. Luo, S. Jiang, and F. Amzajerdian, "Single-frequency narrow-linewidth Tm-doped fiber laser using silicate glass fibe," Opt. Lett. **34**, 3493–3495 (2009).

[20] Z. Zhang, A. J. Boyland, J. K. Sahu, W. A. Clarkson, and M. Ibsen, "High-power single-frequency thulium-doped fiber DBR laser at 1943 nm," IEEE Photonics Technol. Lett. **23**, 417–419 (2011).

[21] X. Wang, P. Zhou, X. Wang, H. Xiao, L. Si, N. Park, J. W. Dawson, K. J. Vahala, C. Miller, C. Yang, S. Xu, S. Mo, C. Li, Z. Feng, D. Chen, Z. Yang, and Z. Jiang, "102 W monolithic single frequency Tm-doped fiber MOPA," Opt. Express **21**, 32386–32392 (2013).

[22] C. W. Rudy, M. J. F. Digonnet, and R. L. Byer, "Advances in 2-μm Tm-doped mode-locked fiber lasers," Opt. Fiber Technol. **20**, 642–649 (2014).

[23] J. Geng, Q. Wang, J. Smith, T. Luo, F. Amzajerdian, and S. Jiang, "All-fiber Q-switched single-frequency Tm-doped laser near 2 um," **34**, 3713–3715 (2009).

[24] E. Lucas, L. Lombard, Y. Jaouën, S. Bordais, and G. Canat, "1 kW peak power, 110 ns single-frequency thulium doped fiber amplifier at 2050 nm," Appl. Opt. **53**, 4413–4419 (2014).

[25] W. Shi, E. B. Petersen, D. T. Nguyen, Z. Yao, A. Chavez-Pirson, N. Peyghambarian, and J. Yu, "220 μJ monolithic single-frequency Q-switched fiber laser at 2 μm by using highly Tm-doped germanate fibers," Opt. Lett. **36**, 3575 (2011).

[26] L. E. Nelson, E. P. Ippen, and H. A. Haus, "Broadly tunable sub-500 fs pulses from an additive-pulse mode-locked thulium-doped fiber ring laser," Appl. Phys. Lett. **67**, (1995).

[27] R. Andrew Sims, P. Kadwani, L. Shah, and M. Richardson, "All thulium fiber CPA system with 107 fs pulse duration and 42 nm bandwidth," Opt. InfoBase Conf. Pap. 4–6 (2011).

[28] X. Zhu and N. Peyghambarian, "High-power ZBLAN glass fiber lasers: Review and prospect," Adv. Optoelectron. **2010**, (2010).

[29] J. Cajzl, P. Peterka, M. Kowalczyk, J. Tarka, G. Sobon, J. Sotor, J. Aubrecht, P. Honzátko, and I. Kašík, "Thulium-Doped Silica fibers with enhanced fluorescence lifetime and their application in ultrafast fiber lasers," Fibers **6**, (2018).

[30] B. M. Walsh and N. P. Barnes, "Comparison of Tm: ZBLAN and Tm: Silica fiber lasers; Spectroscopy and tunable pulsed laser operation around 1.9 μm," Appl. Phys. B Lasers Opt. **78**, 325–333 (2004).

[31] S. D. Jackson and S. Mossman, "Efficiency dependence on the Tm^3+ and Al^3+ concentrations for Tm^3+-doped silica double-clad fiber lasers," Appl. Opt. **42**, 2702 (2003).